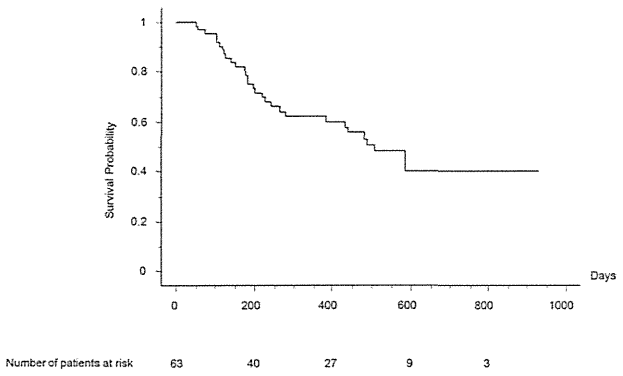

Figure 1. This Kaplan-Meier plot illustrates overall survival for all patients in the study.

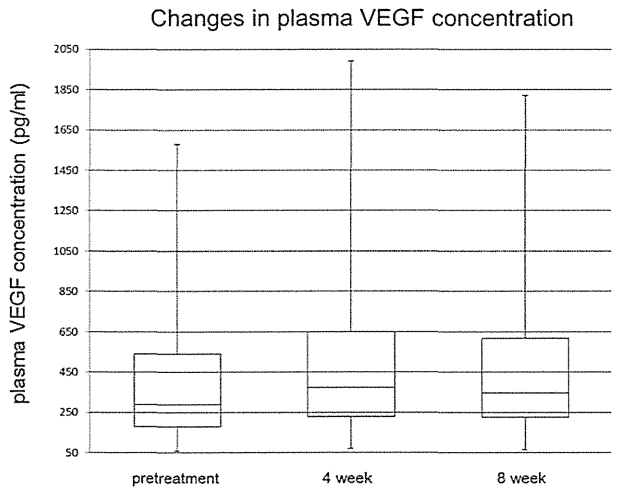

Figure 2. Changes in plasma vascular endothelial growth factor (VEGF) concentrations are illustrated.

(Fig. 1). Plasma VEGF concentrations at baseline, at 4 weeks, and at 8 weeks after the initiation of sorafenib treatment were 288 pg/mL (range, 60-1580 pg/mL), 372 pg/mL (range, 69-1990 pg/mL), and 347 pg/mL (range, 64-1840 pg/mL), respectively (Fig. 2). Plasma VEGF concentrations increased within 4 weeks after the administration of sorafenib in 47 of 63 patients (74.6%). The median survival of patients who had a decrease in their plasma VEGF concentration at week 4 (n = 16) and an increase in their plasma VEGF concentration at week 4 (n = 47) were 19.5 months and 16.8 months, respectively; and there was no significant difference in OS between changes in plasma VEGF at 4 weeks ($P = .645$). However, patients who had a VEGF decrease at week 8 (n = 14) had a longer median survival than those who did not have a VEGF decrease (n = 49; 30.9 months vs 14.4

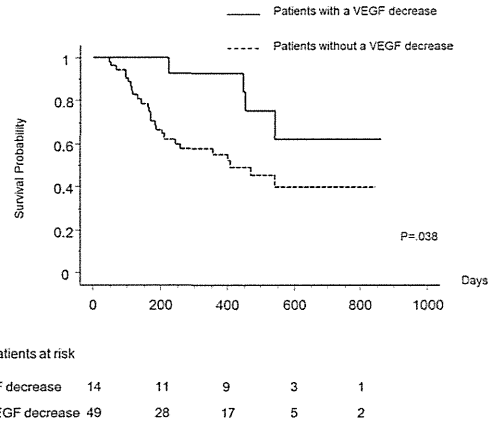

Figure 3. This Kaplan-Meier plot illustrates overall survival according to changes in vascular endothelial growth factor (VEGF) concentration.

months; $P = .038$) (Fig. 3), suggesting that a decrease in VEGF concentration 8 weeks after starting sorafenib treatment is closely associated with a favorable prognosis. The median percentage of decrease in the plasma VEGF concentration was 18.3% (range, 7%-41.7%). There were no differences in any pretreatment patient characteristics, including HCC stage and Child-Pugh score, between patients who did and did not have a VEGF decrease (Table 2).

Relation Between Radiologic Findings or Serum α-Fetoprotein Concentration and Overall Survival

The best radiologic responses to therapy assessed by modified RECIST were classified as a complete response (CR) (n = 4), a partial response (PR) (n = 16), stable disease (SD) (n = 34), and PD (n = 9). Fourteen patients had a VEGF decrease, and their best radiologic responses were a CR (n = 2), a PR (n = 2), SD (n = 9), and PD (n = 1). There was no significant difference in OS between the patients who had an objective response (CR + PR) and those with SD. The survival of patients who had PD was significantly worse than that of the patients without PD (median OS, 5.8 months and 19.4 months, respectively; $P = .0006$). There was no significant difference in OS between patients who had an AFP response and those who did not have an AFP response within the group that did not have PD (ie, those who attained a CR, a PR, or SD [the non-PD group]) (Fig. 4). There also was no significant difference ($P = .111$) between patients who did and did not have an AFP response among those in the non-PD group who had had an elevated AFP at baseline.

TABLE 2. Characteristics of Patients Categorized According to Variation in Vascular Endothelial Growth Factor Levels at 8 Weeks of Sorafenib Treatment

Characteristic	No. of Patients (%)		
	With VEGF Decrease, n = 14	Without VEGF Decrease, n = 49	*P*
Age, y	72	69	.325
Sex: Men	11 (78.6)	42 (85.7)	.679
Body weight, kg	58.3	62.3	.175
Cause of disease			.210
Hepatitis B	0 (0)	8 (16.3)	
Hepatitis C	9 (64.3)	24 (49)	
Other	5 (35.7)	17 (34.7)	
Prior treatment			.797
Yes	11 (78.6)	40 (81.6)	
No	3 (21.4)	9 (18.4)	
Baseline bilirubin, mg/dL	0.8	1.0	.375
Baseline albumin, g/dL	3.4	3.6	.190
Child-Pugh score			.178
5	7 (50)	30 (61.2)	
6	7 (50)	16 (32.7)	
7	0 (0)	3 (6.1)	
Maximum tumor size, cm			.892
≤5	8 (57.1)	22 (44.9)	
>5	6 (42.9)	27 (55.1)	
No. of tumors			.883
≤3	10 (71.4)	34 (69.4)	
>3	4 (28.6)	15 (30.6)	
Extrahepatic disease			.502
Yes	3 (21.4)	15 (30.6)	
No	11 (78.6)	34 (69.4)	
Site of metastatic disease			
Lung	1	7	
Bone	1	4	
Lymph node	1	3	
Lung and bone	0	1	
Major vascular invasion			.739
Yes	3 (21.4)	15 (30.6)	
No	11 (78.5)	34 (69.4)	

Abbreviations: VEGF: vascular endothelial growth factor.

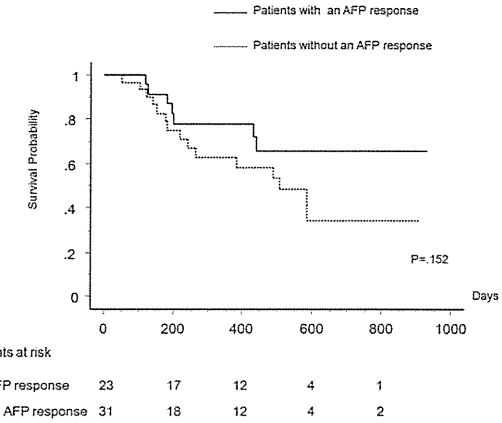

Figure 4. This Kaplan-Meier plot illustrates overall survival according to α-fetoprotein (AFP) response in patients without progressive disease (PD), classified as non-PD (ie, those who had a complete response, a partial response, or stable disease) according to modified Response Evaluation Criteria in Solid Tumors.

It is noteworthy that all patients who had a VEGF decrease and an AFP response survived during the observation period (median, 19.7 months; range, 6.5-31.0 months). In patients without a VEGF response (n = 49), there was no significant difference in OS between those who did and did not have an AFP response ($P = .147$). Of 49 patients who did not have a VEGF decrease at 8 weeks, 19 patients were able to survive beyond 1 year after starting sorafenib. Nine patients without a VEGF decrease at 8 weeks survived for >18 months.

Prognostic Factors After Sorafenib Administration

In univariate analysis, among all patients, a VEGF decease and an AFP response were associated significantly with OS after starting sorafenib. Major vascular invasion and PD, as evidenced by radiologic findings after sorafenib administration, also were significant prognostic factors. To predict which patients would have a highly favorable prognosis, the prognostic factors associated with 1-year survival after starting sorafenib were assessed in univariate and multivariate analyses. In the univariate analysis, a VEGF decrease, PD, and major vascular invasion were associated significantly with survival (Table 3). In the multivariate analysis, which was performed using those factors as covariates, a VEGF decrease was identified as an independent factor associated significantly with survival (Table 3). There was a significant difference in OS among the 3 groups (patients with a VEGF decrease and non-PD, patients without a VEGF decrease but non-PD, and patients without a VEGF decrease and PD; $P = .0013$) (Fig. 5). Only 1 patient who had a VEGF decrease was classified with PD. All 4 patients who had a VEGF decrease and an objective response (CR or PR) were able to survive during the observation period.

Adverse Events During Sorafenib Treatment

The overall incidence of treatment-related adverse events was 100%. The rate of discontinuation of sorafenib as a result of adverse events was 22.2%. Adverse events that led to the discontinuation of sorafenib treatment were liver dysfunction (63.6%), hand-foot skin reaction (18.2%), interstitial pneumonia (9.1%), and rash (9.1%). Dose reductions because of adverse events occurred in 62 patients. The most frequent adverse event leading to dose reductions was liver dysfunction (33.9%). In addition,

TABLE 3. Prognostic Factors Associated With 1-Year Survival After Sorafenib Administration

Risk Factor	OR (95% CI)[a]	*P*
Univariate analysis		
Age, by every 10 y	1.47 (0.75-2.87)	.266
Sex		
Women	1.00	
Men	0.26 (0.50-1.39)	.116
HBV infection		
Negative	1.00	
Positive	0.33 (0.06-2.02)	.231
HCV infection		
Negative	1.00	
Positive	1.23 (0.41-3.74)	.714
Albumin, by every 1 g/dL,	1.34 (0.45-3.99)	.604
Total bilirubin, by every 1 mg/dL	0.79 (0.28-2.25)	.656
Pre-AFP, by every 10 ng/mL	1.00 (1.00-1.00)	.161
Tumor size, cm		
<5	1.00	
≥5	0.42 (0.14-1.32)	.147
No. of tumors		
≤3	1.00	
≥4	0.26 (0.06-1.08)	.064
Major vascular invasion		
Yes	1.00	
No	4.00 (1.12-14.4)	.034
Extrahepatic metastasis		
Yes	1	
No	1.82 (0.56-5.90)	.320
5% VEGF decrease at wk 8		
No	1.00	
Yes	11.1 (1.29-94.6)	.028
PD		
No	1.00	
Yes	0.16 (0.29-0.86)	.033
Objective response: CR + PR		
No	1.00	
Yes	1.63 (0.49-5.42)	.426
AFP response		
No	1.00	
Yes	2.76 (0.80-9.52)	.107
Multivariate analysis[b]		
5% VEGF decrease at wk 8		
No	1.00	
Yes	10.0 (1.02-91.3)	.041
PD		
No	1.00	
Yes	0.20 (0.29-1.39)	.104
Major vascular invasion		
Yes	1.00	
No	3.03 (0.71-12.9)	.134

Abbreviations: AFP, α-fetoprotein; CI, confidence interval; CR, complete response; HBV, hepatitis B virus; HCV, hepatitis C virus; PD, progressive disease; PR, partial response; VEGF, vascular endothelial growth factor.
[a] The ORs for 1-year survival were calculated using logistic regression analysis.
[b] In the multivariate logistic analysis, a 5% VEGF decrease, PD, and portal invasion were included as covariates.

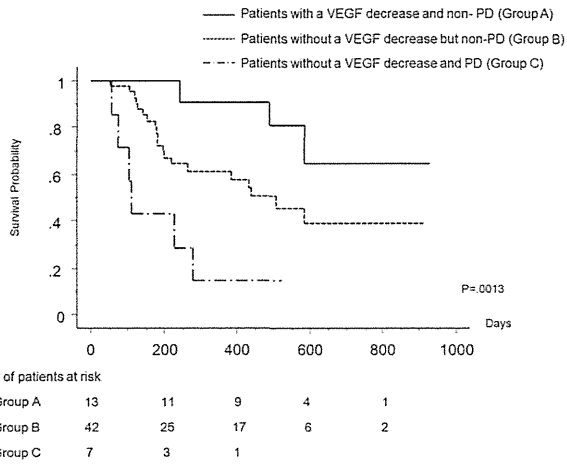

Figure 5. This Kaplan-Meier plot illustrates overall survival according to the combination of vascular endothelial growth factor (VEGF) changes and radiologic findings classified by modified Response Evaluation Criteria in Solid Tumors. Non-PD indicates patients who did not have progressive disease (PD) (ie, those who had a complete response, a partial response, or stable disease).

the incidence of adverse events was not related to plasma VEGF concentrations.

DISCUSSION

In the current study, we demonstrated that plasma VEGF concentrations change dynamically during sorafenib therapy, and changes in VEGF concentration are closely associated with OS in patients who receive treatment with sorafenib. VEGF is the major mediator of angiogenesis in HCC, and several studies have correlated VEGF concentrations with the prognosis of patients who have advanced HCC.[5,14-21]

Recently, a new staging system was proposed that includes the plasma VEGF concentration along with the Cancer of the Liver Italian Program (CLIP) score; this new system—known as the V-CLIP score—classifies patients with advanced HCC more appropriately into a homogeneous prognostic group.[22] Therefore, the concentration of circulating VEGF is included as a candidate prognostic marker for HCC, especially in patients with advanced disease. The objective of our study was to elucidate the important question of whether an on-treatment change in VEGF is a potentially useful new biomarker for predicting prognosis in patients who survive beyond 8 weeks, because such an on-treatment predictor among patients who have relatively longer survival has not yet been elucidated. In this study, plasma VEGF concentrations increased from pretreatment levels within 4 weeks of starting sorafenib in 47 of 63 patients (74.6%). This was followed by a decrease in plasma VEGF levels at 8 weeks in 68.1% of patients. A possible mechanism of this transient increase in VEGF after starting sorafenib may be related to a reactive increase against the inhibition of VEGF activity or hypoxia induced by sorafenib. This

hypothesis is supported by the demonstration that plasma VEGF concentrations increased shortly after treatment with TACE.[24-26] It is believed that these increases in plasma VEGF concentration are related to the induction of tissue hypoxia.[27] However, the peak time point of VEGF elevation during sorafenib administration was different from that previously reported in TACE, in which a transient elevation of VEGF was observed within 7 days after TACE.[24-26] This observed difference may be related to the continuous induction of hypoxia by sorafenib administration.

It is noteworthy that, in our study, decreases in plasma VEGF observed within 8 weeks of sorafenib administration were associated with better OS. One possible reason for this association may be that the decrease in VEGF concentrations reflects a decrease in the number of tumor cells secreting VEGF. An association between changes in VEGF concentrations and disease progression was observed in a previous study of an anti-VEGF antibody, bevacizumab, in patients with advanced HCC.[23] In that study, plasma VEGF-A concentrations decreased from baseline in all patients after 8 weeks of bevacizumab therapy and increased to near baseline levels in 5 of 6 patients at the time of disease progression. Unfortunately, plasma VEGF-A levels after 8 weeks of bevacizumab in that study were available for only 8 of 46 patients who were enrolled the study, and plasma VEGF-A levels after 4 weeks were not evaluated. In our study, all patients were evaluated before and every 4 weeks after starting sorafenib. Moreover, we demonstrated the usefulness of plasma VEGF concentrations at 8 weeks and not at 4 weeks. Zhu et al[28] reported that plasma levels of VEGF and placental growth factor increased after cediranib, a pan-VEGFR tyrosine kinase inhibitor monotherapy for advanced HCC. In that study, progression-free survival was correlated inversely with baseline levels of VEGF, soluble VEGFR2 (sVEGFR2), and basic fibroblast growth factor and with on-treatment levels of basic fibroblast growth factor and insulin-like growth factor-1; and progression-free survival was directly associated with on-treatment levels of interferon-γ. Because changes of VEGF concentrations during therapy were not identified as a prognostic factor in the study by Zhu et al, biomarkers that predict prognosis may be different among different types of tyrosine kinase inhibitors. Jayson et al[29] reported that plasma VEGF-A in patients who received bevacizumab was potentially predictive and prognostic in metastatic breast, gastric, and pancreatic cancers; however, it was only prognostic (and not predictive) in metastatic colorectal cancer, nonsmall cell lung cancer, and renal cell carcinoma. In our study, we measured plasma VEGF concentrations and not plasma VEGF-A concentrations. Sorafenib is a multikinase inhibitor, whereas bevacizumab is a humanized monoclonal antibody that recognizes and blocks VEGF-A expression. Further studies to evaluate the clinical usefulness of determining VEGF and VEGF-A concentrations during sorafenib therapy are necessary in various cancers. Although the precise mechanism underlying the association between serial changes in VEGF and disease progression is unclear, the findings of the current study are extremely valuable for clinical practice in predicting the prognosis of patients who receive treatment with sorafenib.

Llovet et al[5] studied plasma biomarkers as predictors of outcome in patients with advanced HCC. They measured plasma biomarkers in 491 patients at baseline and in 305 patients after 12 weeks in a phase 3, randomized, controlled trial (the SHARP trial). Those authors concluded that angiopoietin-2 and VEGF were independent predictors of survival in patients with advanced HCC and that none of the tested biomarkers significantly predicted response to sorafenib. In our study, by measuring plasma VEGF monthly, we demonstrated that the changes 8 weeks after starting sorafenib were important for predicting OS.

It has been reported that modified RECIST guidelines are useful for predicting efficacy and prognosis after patients with advanced HCC receive treatment with sorafenib.[30] However, modified RECIST can only be used for typical hypervascular HCC, and not for atypical HCC, including poorly differentiated HCC and diffuse-type HCC. Moreover, the percentage of patients in our study who had PD was only 11.1% (9 of 63 patients), and the objective response rate (CR + PR vs SD) could not predict OS, suggesting that using only modified RECIST guidelines was insufficient for predicting OS in most patients who received sorafenib (non-PD patients). Therefore, it is important to identify a predictive biomarker for those patients who can expect long survival during sorafenib therapy, although their radiologic findings may not be categorized as objective responses.

From this point of view, decreases in VEGF observed in non-PD patients at week 8 may identify patients who have a favorable prognosis. According to our results, the median survival of patients who had a VEGF decrease was extremely good at 31.0 months, and we demonstrated that a VEGF decrease, but not modified RECIST or AFP, was the only significant post-therapeutic factor associated with favorable survival after sorafenib administration (Table 3). In our study, all

patients who had both a VEGF decrease and an AFP response survived during the observation period (median, 19.7 months). Taken together, the combination of a plasma VEGF decrease, an AFP response, and modified RECIST is useful for predicting an extremely favorable prognosis.

This study had a few limitations. The first was our subanalysis of consecutive patients. However, the median survival for the 23 excluded patients who were available for estimation was equivalent to that of the included patients (16.8 months); therefore, it is unlikely that selection bias affected our results. The second limitation is that we measured only plasma VEGF concentrations. In previous studies, many factors, including VEGF-A, short VEGF-A isoform, sVEGFR1, sVEGFR2, sVEGFR3, angiopoietin-2, and insulin-like growth factor-2, were evaluated as biomarkers. However, to our knowledge, this is the first clinical study to demonstrate the early dynamic changes in plasma VEGF concentrations in patients who received sorafenib. Finally, the number of patients in this study was relatively small to make recommendations to physicians. Our results indicated that patients who have decreased VEGF concentrations at 8 weeks have a favorable prognosis, regardless of their radiologic findings. However, further studies with a larger number of patients will be necessary to propose new recommendations.

In conclusion, changes in plasma VEGF concentrations during sorafenib treatment are dynamic in patients with advanced HCC, and an observed decrease in the plasma VEGF concentration 8 weeks after starting sorafenib is associated significantly with favorable OS. Today, because many clinical trials of new molecular-targeted agents for HCC are being conducted, it is necessary for hepatologists and oncologists to determine the time when alternative agents should be started as a second or third line of treatment. Our results have potentially important clinical implications for physicians and may influence their decisions regarding a treatment strategy for advanced HCC in individual patients.

FUNDING SUPPORT

This work was supported by grants from the Japanese Ministry of Welfare, Health, and Labor.

CONFLICT OF INTEREST DISCLOSURES

Yasuhiro Asahina received grants from the Japanese Ministry of Welfare, Health, and Labor and the Japanese Ministry of Education, Culture, Sports, and Science during the conduct of this study. Dr. Asahina has also received grants from Chugai Pharmaceutical Company, Ltd.; Toray Industries, Inc.; Bristol-Myers Squibb; Dainippon Sumitomo Pharma Company, Ltd.; Merck Sharp & Dohme (MSD); and Daiichi Sankyo Company, Ltd., and has received lecture fees from Chugai Pharmaceutical Company, Ltd. and MSD. Nobuyuki Enomoto has received grants and consulting fees from Bayer, Chugai-Roche, MDS, Bristol-Myers Squibb, and GlaxoSmithKline. Namiki Izumi has received lecture fees from MSD, Chugai Pharmaceutical Company, Ltd.; Daiichi-Sankyo Company, Ltd.; Bayer AG; and Bristol-Myers Squibb.

REFERENCES

1. World Health Organization, International Agency for Research on Cancer (IARC); Boyle P, Levin B, eds. World Cancer Report 2008. Lyon, France: IARC Press; 2008.
2. European Association for the Study of the Liver, European Organisation for Research and Treatment of Cancer. EASL-EORTC Clinical Practice Guidelines: management of hepatocellular carcinoma. *J Hepatol.* 2012;56:908-943.
3. Llovet JM, Ricci S, Mazzaferro V, et al. SHARP Investigators Study Group. Sorafenib in advanced hepatocellular carcinoma. *N Engl J Med.* 2008;359:378-390.
4. Cheng AL, Kang YK, Chen Z, et al. Efficacy and safety of sorafenib in patients in the Asia-Pacific region with advanced hepatocellular carcinoma: a phase III randomized, double-blind, placebo-controlled trial. *Lancet Oncol.* 2009;10:25-34.
5. Llovet JM, Pena CE, Lathia CD, Shan M, Meinhardt G, Bruix J. Plasma biomarkers as predictors of outcome in patients with advanced hepatocellular carcinoma. *Clin Cancer Res.* 2012;18: 2290-3000.
6. Lencioni R, Llovet JM. Modified RECIST (mRECIST) assessment for hepatocellular carcinoma. *Semin Liver Dis.* 2010;30:52-60.
7. Shao YY, Lin ZZ, Hsu C, Shen CH, Cheng AL. Early alpha-fetoprotein response predicts treatment efficacy of antiangiogenic systemic therapy in patients with advanced hepatocellular carcinoma. *Cancer.* 2010;116:4590-4596.
8. Kuzuya T, Asahina Y, Tsuchiya K, et al. Early decrease in α-fetoprotein, but not des-γ-carboxy prothrombin, predicts sorafenib efficacy in patients with advanced hepatocellular carcinoma. *Oncology.* 2011;81:251-258.
9. Personeni N, Bozzarelli S, Pressiani T, et al. Usefulness of alpha-fetoprotein response in patients treated with sorafenib for advanced hepatocellular carcinoma. *J Hepatol.* 2012;57:101-107.
10. Raoul JL, Bruix J, Greten TF, et al. Relationship between baseline hepatic status and outcome, and effect of sorafenib on liver function: SHARP trial subanalyses. *J Hepatol.* 2012;56:1080-1088.
11. Hora C, Romanque P, Dufour JF. Effect of sorafenib on murine liver regeneration. *Hepatology.* 2011;53:577-586.
12. Kudo M, Izumi N, Kokudo N, Matsui O, Sakamoto M, Makuuchi M. Management of hepatocellular carcinoma in Japan: consensus-based clinical practice guidelines proposed by the Japan Society of Hepatology (JSH) 2010 updated version. *Dig Dis.* 2011;29:339-364.
13. Bruix J, Sherman M; American Association for the Study of Liver Diseases. Management of hepatocellular carcinoma: an update. *Hepatology.* 2011;53:1020-1022.
14. El-Assal ON, Yamanoi A, Soda Y, et al. Clinical significance of microvessel density and vascular endothelial growth factor expression in hepatocellular carcinoma and surrounding liver: possible involvement of vascular endothelial growth factor in the angiogenesis of cirrhotic liver. *Hepatology.* 1998;27:1554-1562.
15. Yamaguchi R, Yano H, Iemura A, Ogasawara S, Haramaki M, Kojiro M. Expression of vascular endothelial growth factor in human hepatocellular carcinoma. *Hepatology.* 1998;28:68-77.
16. Yoshiji H, Kuriyama S, Yoshii J, et al. Synergistic effect of basic fibroblast growth factor and vascular endothelial growth factor in murine hepatocellular carcinoma. *Hepatology.* 2002;35:834-842.
17. Tamesa T, Iizuka N, Mori N, et al. High serum levels of vascular endothelial growth factor after hepatectomy are associated with poor prognosis in hepatocellular carcinoma. *Hepatogastroenterology.* 2009; 56:1122-1126.
18. Hu J, Xu Y, Shen ZZ, et al. High expressions of vascular endothelial growth factor and platelet-derived endothelial cell growth factor

predict poor prognosis in alpha-fetoprotein-negative hepatocellular carcinoma patients after curative resection. *J Cancer Res.* 2009;135: 1359-1367.
19. Poon RT, Lau C, Pang R, Ng KK, Yuen J, Fan ST. High serum vascular endothelial growth factor levels predict poor prognosis after radiofrequency ablation of hepatocellular carcinoma: importance of tumor biomarker in ablative therapies. *Ann Surg Oncol.* 2007;14: 1835-1845.
20. Schoenleber SJ, Kurtz DM, Talwalkar JA, Rober LR, Gores GJ. Prognostic role of vascular endothelial growth factor in hepatocellular carcinoma: systemic review and meta-analysis. *Br J Cancer.* 2009; 100:1385-1392.
21. Kaseb AO, Hanbali A, Cotant M, Hassan MM, Wollner I, Philip PA. Vascular endothelial growth factor in the management of hepatocellular carcinoma: a review of literature. *Cancer.* 2009;115: 4895-4906.
22. Kaseb A, Hassan M, Lin E, Xiao L, Kumar V, Morris J. V-CLIP: integrating plasma vascular endothelial growth factor into a new scoring system to stratify patients with advanced hepatocellular carcinoma for clinical trials. *Cancer.* 2011;117:2478-2488.
23. Siegel AB, Cohen EI, Ocean A, et al. Phase II trial evaluating the clinical and biologic effects of bevacizumab in unresectable hepatocellular carcinoma. *J Clin Oncol.* 2008;26:2992-2998.
24. Li X, Feng GS, Zheng CS, Zhuo CK, Liu X. Expression of plasma vascular endothelial growth factor in patients with hepatocellular carcinoma and effect of transcatheter arterial chemoembolization therapy on plasma vascular endothelial growth factor level. *World J Gastroenterol.* 2004;10:2878-2882.
25. Suzuki H, Mori M, Kawaguchi C, Adachi M, Miura S, Ishii H. Serum vascular endothelial growth factor in the course of transcatheter arterial embolization of hepatocellular carcinoma. *Int J Oncol.* 1999; 14:1087-1090.
26. Shim JH, Park JW, Kim JH, et al. Association between increment of serum VEGF and poor prognosis after transcatheter arterial chemoembolization in hepatocellular carcinoma patients. *Cancer Sci.* 2008;99:2037-2044.
27. von Marschall Z, Cramer T, Hocker M, Finkenzeller G, Wiedenmann B, Rosewicz S. Dual mechanism of vascular endothelial growth factor upregulation by hypoxia in human hepatocellular carcinoma. *Gut.* 2001;48:87-96.
28. Zhu AX, Ancukiewicz M, Duda DG, et al. Efficacy, safety, pharmacokinetics, and biomarkers of cediranib monotherapy in advanced hepatocellular carcinoma: a phase II study. *Clin Cancer Res.* 2013; 19:1557-1566.
29. Jayson GC, de Haas S, Delmar P, et al. Evaluation of plasma VEGF-A as a potential predictive pan-tumour biomarker for bevacizumab. Abstract 804. Paper presented at: 2011 European Multidisciplinary Cancer Congress; Stockholm, Sweden; September 23-27, 2011.
30. Edeline J, Boucher E, Rolland Y, et al. Comparison of tumor response by Response Evaluation Criteria in Solid Tumors (RECIST) and modified RECIST in patients treated with sorafenib for hepatocellular carcinoma. *Cancer.* 2012;118:147-156.

OPEN ACCESS Freely available online

PLOS ONE

Inhibitory Effects of Caffeic Acid Phenethyl Ester Derivatives on Replication of Hepatitis C Virus

Hui Shen[1], Atsuya Yamashita[1], Masamichi Nakakoshi[2], Hiromasa Yokoe[3], Masashi Sudo[3], Hirotake Kasai[1], Tomohisa Tanaka[1], Yuusuke Fujimoto[1], Masanori Ikeda[4], Nobuyuki Kato[4], Naoya Sakamoto[5], Hiroko Shindo[6], Shinya Maekawa[6], Nobuyuki Enomoto[6], Masayoshi Tsubuki[3]*, Kohji Moriishi[1]*

1 Department of Microbiology, Division of Medicine, Graduate School of Medicine and Engineering, University of Yamanashi, Yamanashi, Japan, **2** Faculty of Pharmaceutical Sciences, Toho University, Chiba, Japan, **3** Institute of Medical Chemistry, Hoshi University, Tokyo, Japan, **4** Department of Tumor Virology, Okayama University Graduate School of Medicine, Dentistry, and Pharmaceutical Sciences, Okayama, Japan, **5** Department of Gastroenterology and Hepatology, Hokkaido University Graduate School of Medicine, Sapporo, Japan, **6** First Department of Internal Medicine, Faculty of Medicine, University of Yamanashi, Yamanashi, Japan

Abstract

Caffeic acid phenethyl ester (CAPE) has been reported as a multifunctional compound. In this report, we tested the effect of CAPE and its derivatives on hepatitis C virus (HCV) replication in order to develop an effective anti-HCV compound. CAPE and CAPE derivatives exhibited anti-HCV activity against an HCV replicon cell line of genotype 1b with EC_{50} values in a range from 1.0 to 109.6 μM. Analyses of chemical structure and antiviral activity suggested that the length of the n-alkyl side chain and catechol moiety are responsible for the anti-HCV activity of these compounds. Caffeic acid n-octyl ester exhibited the highest anti-HCV activity among the tested derivatives with an EC_{50} value of 1.0 μM and an SI value of 63.1 by using the replicon cell line derived from genotype 1b strain Con1. Treatment with caffeic acid n-octyl ester inhibited HCV replication of genotype 2a at a similar level to that of genotype 1b irrespectively of interferon signaling. Caffeic acid n-octyl ester could synergistically enhance the anti-HCV activities of interferon-alpha 2b, daclatasvir, and VX-222, but neither telaprevir nor danoprevir. These results suggest that caffeic acid n-octyl ester is a potential candidate for novel anti-HCV chemotherapy drugs.

Citation: Shen H, Yamashita A, Nakakoshi M, Yokoe H, Sudo M, et al. (2013) Inhibitory Effects of Caffeic Acid Phenethyl Ester Derivatives on Replication of Hepatitis C Virus. PLoS ONE 8(12): e82299. doi:10.1371/journal.pone.0082299

Editor: Hak Hotta, Kobe University, Japan

Received September 15, 2013; **Accepted** October 31, 2013; **Published** December 17, 2013

Funding: This work was supported in part by grants-in-aid from the Ministry of Health, Labor, and Welfare and from the Ministry of Education, Culture, Sports, Science, and Technology of Japan. The funders had no role in study design, data collection and analysis, decision to publish, or preparation of the manuscript.

Competing Interests: The authors have declared that no competing interests exist.

* E-mail: tsubuki@hoshi.ac.jp (MT); kmoriishi@yamanashi.ac.jp (KM)

Introduction

Hepatitis C virus (HCV) is well known as a major causative agent of chronic liver disease including cirrhosis and hepatocellular carcinoma and is thought to persistently infect 170 million patients worldwide [1]. HCV belongs to the genus *Hepacivirus* of the family *Flaviviridae* and possesses a viral genome that is characterized by a single positive strand RNA with a nucleotide length of 9.6 kb [2]. The single polypeptide coded by the genome is composed of 3,000 amino acids and is cleaved by host and viral proteases, resulting in 10 proteins, which are classified into structural and nonstructural proteins [3]. The viral genome is transcribed by a replication complex consisting of NS3 to NS5B and host factors [4]. NS3 forms a complex with NS4A and becomes a fully active form to cleave the C-terminal parts of the nonstructural proteins. The advanced NS3/4A protease inhibitors, telaprevir and boceprevir, have been employed in the treatment of chronic hepatitis C patients infected with genotype 1 [5]. Sustained virologic response (SVR) was reportedly 80% in patients infected with genotype 1 following triple combination therapy with pegylated interferon, ribavirin, and telaprevir [6], although the therapy exhibits side effects including rash, severe cutaneous eruption, influenza-like symptoms, cytopenias, depression, and anemia [7]. In addition, there is the possibility of the emergence of drug-resistant viruses following treatment with those anti-HCV drugs [8] Thus, further study is required for development of safer and more effective anti-HCV compounds.

Several recent reports indicate that silbinin [9], epigallocatechin-3-gallate [10], curcumin [11], quercetin [12] and proanthocyanidins [13], which all originate from natural sources, have exhibited inhibitory activity against HCV replication in cultured cells. Caffeic acid phenethyl ester (CAPE) is an active component included in propolis prepared from honeybee hives, and has a similar structure to flavonoids (Fig. 1A). CAPE has multifunctional properties containing anti-inflammatory [14], antiviral [15], anticarcinogenic [16], and immunomodulatory activities [15]. CAPE also inhibits enzymatic activities of endogenous and viral proteins [17–19] and transcriptional activity of NF-kappaB [14,20]. In addition, CAPE could suppress HCV replication enhanced by using the NF-kappaB activation activity of morphine [21], although it has been unknown which of moieties including CAPE is responsible for anti-HCV activity. Furthermore, it is not clear whether chemical modification of CAPE could enhance anti-HCV activity or not. In this report, we examined the effect of

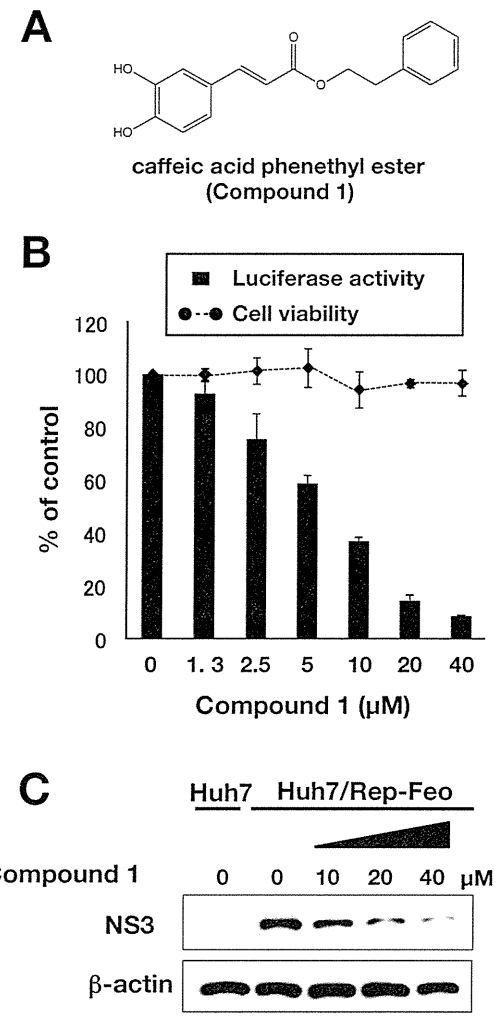

Figure 1. Effect of CAPE on viral replication in the replicon cell line of genotype 1b. (A) Molecular structure of CAPE. (B) Huh7/Rep-Feo cells were incubated for 72 h in a medium containing various concentrations of CAPE. Luciferase and cytotoxicity assays were carried out by the method described in Materials and Methods. Error bars indicate standard deviation. The data represent results from three independent experiments. (C) Protein extract was prepared from Huh7/Rep-Feo cells treated for 72 h with the indicated concentration of CAPE and it was then was subjected to Western blotting using antibodies to NS3 and beta-actin.
doi:10.1371/journal.pone.0082299.g001

CAPE derivatives on HCV proliferation to develop more effective and safer anti-HCV compounds.

Results

Effect of CAPE on HCV RNA replication in HCV subgenomic replicon cells

CAPE is composed of ester of caffeic acid and phenethyl alcohol (Fig. 1A). We examined the effect of CAPE (compound **1**) on both viral replication and cell growth in the HCV subgenomic replicon cell line Huh7/Rep-Feo. The replicon cell line was treated with various concentrations of compound **1**. The replication level of the HCV RNA was measured as an enzymatic activity of luciferase, which is bicistronically, encoded on the replicon RNA. Compound **1** suppressed HCV RNA replication at concentrations from 1.3 to 40 μM in a dose-dependent manner, but did not affect cell viability (Fig. 1B). HCV NS3, which is a viral protease, was decreased at the protein level by treatment with CAPE in a dose-dependent manner, corresponding to the viral replication, whereas beta-actin was not changed in the replicon cell line (Fig. 1C). Based on the calculation using a dose dependency of CAPE, compound **1** exhibited an EC_{50} value of 9.0 μM and a CC_{50} value of 136.1 μM, giving a selectivity index estimate (SI) of 17.9 (Table 1). These results suggest that treatment with CAPE inhibits HCV replication in HCV subgenomic replicon cells.

Structure-activity relationship of CAPE analogues

To clarify the structure-activity relationship of CAPE analogues, we examined the effect of hydroxyl groups on the aromatic ring (catechol moiety), the alkenyl moieties on alpha, beta-unsaturated esters, and the ester parts as follows (Figure S1).

We tested whether commercially available CAPE-related compounds **2** to **6** (Fig. S1) affected HCV replication (Table 1). All these compounds showed weaker inhibitory activity than CAPE (**1**), but are not toxic. Compound **2**, which is the acid component of CAPE, showed a slightly lower value of EC_{50} than compound **3**, which is the compound **2** derivative replaced a hydroxyl group with a methoxyl group of catechol moiety, while compound **4**, which is the derivative lacking two hydroxyl groups within catechol moiety, exhibits a higher value of EC_{50} than compounds **1** and **2**. These data suggest that the catechol moiety of CAPE is required for anti-HCV activity. Interestingly, compounds **5** and **6**, which are natural products including polyhydroxylated acid moieties in the ester parts, showed much weaker inhibitions than compound **1** and exhibits low *Clog P* values. The position of hydroxyl group or/and the structure of the ester part may affect the inhibitory activity and/or hydrophobicity.

We next examined the effects of caffeic acid ester compounds **7** to **11**, which include various lengths of alkyl side chains, on HCV replication (Table 2 and Figure S2). The EC_{50} values decreased in the order methyl ester (compound **7**), n-butyl ester (compound **8**), n-hexyl ester (compound **9**), and n-octyl ester (compound **10**), suggesting that elongation of the n-alkyl side chain increased the inhibitory activity. However, the EC_{50} value of n-dodecyl ester (compound **11**) was higher than that of compound **10**. Thus, n-octyl ester (compound **10**) showed the lowest EC_{50} value and the highest SI among the tested compounds shown in Tables 1 and 2. Compounds **7** to **11** gradually increased own *Clog P* values,

Table 1. Effect of CAPE (**1**) and related compounds **2–6** on HCV replication.

Compound (Number)	EC_{50} [a] (μM)	CC_{50} [b] (μM)	SI [c]	*Clog P* [d]
CAPE (**1**)	9.0±0.7	136.1±1.9	17.9	3.30
caffeic acid (**2**)	36.6±6.7	>320	>8.7	0.98
ferulic acid (**3**)	71.9±5.8	>320	>4.5	1.42
cinnamic acid henethyl ester (**4**)	86.1±6.3	>320	>3.7	4.56
chlorogenic acid (**5**)	103.0±3.4	>320	>3.1	−0.96
rosmarinic acid (**6**)	109.6±1.1	>320	>2.9	1.10

a: Fifty percent effective concentration based on the inhibition of HCV replication.
b: Fifty percent cytotoxicity concentration based on the reduction in cell viability.
c: Selectivity index (CC_{50}/EC_{50}).
d: Determined with ChemDraw software (Chem Bio Office Ultra, 2008).
doi:10.1371/journal.pone.0082299.t001

corresponding to length of n-alkyl side chain (Fig. 2A). Compounds **10** and **11** exhibit EC_{50} values of 2.7 and 5.9 μM, respectively, SI values of 29.6 and 9.80, respectively, and *C*log *P* values of 4.90 and 5.96, respectively, suggesting that high hydrophobic property of n-alkyl side chain decreases anti-HCV activity. The appropriate *C*log *P* value of caffeic acid ester containing unsaturated side chain may be around 5.

Dihydrocaffeic acid methyl ester (compound **12**) showed less activity than caffeic acid methyl ester (compound **7**) regardless of values of *C*log *P* value and CC_{50}, suggesting that the alpha, beta-unsaturated part attached to ester affects the anti-HCV activity level (Table 3 and Figure S3).

We further examined the effect of the hydroxyl groups on the aromatic ring on HCV replication (Table 4 and Figure S4). The EC_{50} values of *O*-methylated caffeic acid n-octyl esters (compounds **13** and **14**) were higher than that of compound **10**. Compounds **15** including 3, 4-di-*O*-methylated caffeic acid n-octyl ester exhibited higher EC_{50} than values of compounds **10**, **13** and **14**. However, addition of a third hydroxyl group to 3, 4, 5-trihydroxy derivative (compound **16**) of compound **10** resulted in a reduction of anti-HCV activity. Furthermore, *C*log *P* values of compound **10**, **13**, **14, 15** and **16** were not correlated with anti-HCV activity (EC_{50} value) (Fig. 2B). These results suggest that the catechol moiety plays an important role in anti-HCV activity, and that the 4-hydroxy moiety is more important for the activity than the 3-hydroxy moiety.

Thus, compound **10**, which exhibits the lowest EC_{50} value and the highest SI value, is the most effective compound among CAPE analogues used in this study.

Effect of CAPE derivatives on virus production

The structure of compound **10** is shown in Fig. 3A. Treatment with compound **10** reduced HCV replication and NS3 protein in a dose-dependent manner at a higher anti-HCV level than

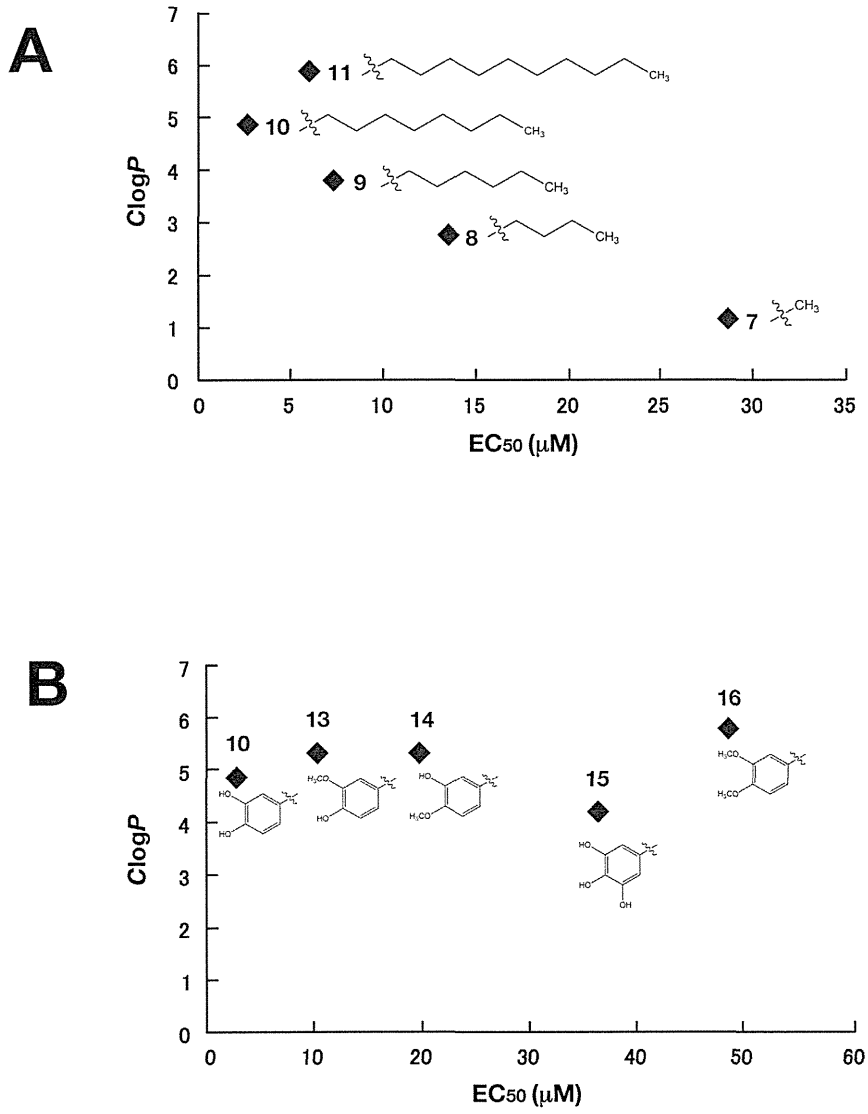

Figure 2. Correlation between the inhibitory effect on HCV replication *and* *C*log *P* of CAPE analogues. Values of *x*-axis indicate EC_{50} values of CAPE analogues, while values of *y*-axis show *C*log *P* values. (A) Correlation between the inhibitory effect on HCV replication and *C*log *P* of CAPE analogues (Compound 7–11). (B) Correlation between the inhibitory effect on HCV replication and *C*log *P* of CAPE analogues (Compound 10 and 13–16).
doi:10.1371/journal.pone.0082299.g002

Table 2. Effect of caffeic acid esters **7, 9–14**, including **1**, on HCV replication.

Compound No.	R	EC_{50} [a] (μM)	CC_{50} [b] (μM)	SI [c]	Clog *P* [d]
7	CH_3	28.6±1.2	122.1±5.0	4.2	1.20
8	C_4H_9	13.5±2.1	39.0±1.1	2.9	2.79
9	C_6H_{13}	7.3±0.2	37.6±1.2	5.1	3.85
10	C_8H_{17}	2.7±0.1	71.7±8.5	26.6	4.90
11	$C_{10}H_{21}$	5.9±0.9	57.9±2.9	9.8	5.96
1	$(CH_2)_2Ph$	9.0±0.7	136.1±1.9	17.9	3.30

The basic structure and side moieties are shown in Figure S2.
a: Fifty percent effective concentration based on the inhibition of HCV replication.
b: Fifty percent cytotoxicity concentration based on the reduction in cell viability.
c: Selectivity index (CC_{50}/EC_{50}).
d: Determined with ChemDraw software (Chem Bio Office Ultra, 2008).
doi:10.1371/journal.pone.0082299.t002

compound **1** (Figs. 3B and C), but not effect enzymatic activities of firefly and *Renilla* luciferases (Fig. 3D) and IRES-dependent translation (Fig. 3E), suggesting that inhibition of HCV replication by compound **10** is not due to offtarget effect. We evaluated the inhibitory effect of compound **10** on three different subgenomic replicon cell lines (1b: N strain, Con1 strain, 2a: JFH-1 strain) and one full genome replicon cell line (1b: O strain). Compound **10** inhibited the viral replication of all replicon cell lines at similar level, and exhibited the lowest EC_{50} value of 1.0 μM and an SI value of 63.1 by using Con1 replicon cells (Table 5). We next examined the effect of compound **10** on virus production by using HCVcc, since subgenomic replicon mimics HCV replication, but not the whole viral cycle. The Huh7 OK1 cell line, which is highly permissive to the HCV JFH1 strain [22], was infected with HCVcc and then treated with compound **10** at 24 h post-infection. The supernatant was harvested 72 h post-infection from the culture supernatant and then the RNA that prepared from the supernatant was estimated by real time qRT-PCR. Figure 3F shows that treatment with compound **10** reduced HCV viral production ($EC_{50} = 1.8 \pm 0.4$ μM) in a similar way to the data obtained by using a replicon cell line. To clarify whether or not compound **10** inhibited HCV replication via interferon-signaling pathway, we analyzed ISRE activity and the expression of interferon stimulated gene (ISG) by using reporter assay and RT-PCR, respectively. The replicon cells were harvested at 48 h post-treatment. There were no significant effects of compound **1**, **6** and **10** on ISRE-promoter activities, while interferon alpha 2b significantly enhanced it as a positive control (Fig.4 A). The data of the RT-PCR analysis showed that the transcriptional expressions of ISGs including Mx1, MxA, IFIT4, ISG15, OAS1, OAS2, and OAS3 were induced with interferon alpha 2b, but not with compound **1**, **6** and **10** (Fig. 4B). These data suggest that the CAPE derivatives have an inhibitory effect on virus production and replication, irrespective of interferon signaling induction.

Synergistic effect of caffeic acid n-octyl ester on interferon and direct-acting antiviral agents

To estimate the effects of drug combinations on anti-HCV activity, we examined the antiviral activity of compound **10** in combination with IFN-α 2b, telaprevir (NS3 protease inhibitor), danoprevir (NS3 protease inhibitor), daclatasvir (NS5A inhibitor) or VX-222 (NS5B polymerase inhibitor). Con1 LUN Sb #26 replicon cells were treated with compound **10** in combination with

Table 3. Effect of caffeic acid esters **7**and **8** on HCV replication.

Compound No.	EC_{50} [a] (μM)	CC_{50} [b] (μM)	SI [c]	Clog *P* [d]
7	28.6±1.2	122.1±5.0	4.2	1.20
12	77.0±1.6	140.7±3.4	1.8	1.02

Chemical structures of both compounds are shown in Figure S3
a: Fifty percent effective concentration based on the inhibition of HCV replication.
b: Fifty percent cytotoxicity concentration based on the reduction in cell viability.
c: Selectivity index (CC_{50}/EC_{50}).
d: Determined with ChemDraw software (Chem Bio Office Ultra, 2008).
doi:10.1371/journal.pone.0082299.t003

each anti-HCV agent at various concentration rations for 72 h. The effect of each drug combination on HCV replication was analyzed by using CalcuSyn. An explanatory diagram of isobologram was shown at a right end of lower panels of Fig. 5A as described in Materials and Methods. As shown in the resulting isobologram, all plots of the calculated EC_{90} values of compound **10** with IFN-alpha 2b, daclatasvir, or VX-222 are located under the additive line, while the plots of compound **10** with telaprevir, or danoprevir are located above the additive line and closed to the additive line (Fig. 5A). Additionally, we determined the degree of inhibition for each drug combination was analyzed as the combination index (CI) calculation at 50, 75 and 90% of effective concentrations by using CalcuSyn. An explanatory diagram was shown at a right end of lower panels of Fig. 5B as described in Materials and Methods. On the basis of the CalcuSyn analysis, the combination of compound **10** with daclatasvir exhibited strong synergistic effect on inhibition of HCV replication in the replicon cells (Fig. 5B, upper middle). The combination of compound **10** with VX-222 exhibited an additive to synergistic effect, suggesting that it trends toward synergistic (Fig. 5B, upper right), and with IFN-alpha 2b exhibited an antagonistic to synergistic effect, suggesting that it trends toward synergistic (Fig. 5B, upper left). In contrast, the combination of compound **10** with telaprevir resulted in antagonistic effect (Fig. 5B, lower left), and with danoprevir resulted in an antagonistic to additive effect, suggesting it trends toward antagonistic (Fig. 5B, lower middle). These calculated data

Table 4. Effect of octyl esters **10** and **13–16** on HCV replication.

Compound No.	R^1, R^2, R^3	EC_{50} [a] (μM)	CC_{50} [b] (μM)	SI [c]	Clog *P* [d]
10	$R^1=R^2=R^3=H$	2.7±0.1	71.7±8.5	26.6	4.90
13	$R^1=CH_3$, $R^2=R^3=H$	10.2±1.1	60.3±1.6	5.9	5.35
14	$R^1=R^3=H$, $R^2=CH_3$	19.6±0.8	59.2±1.4	3	5.35
15	$R^1=R^2=CH_3$, $R^3=H$	48.5±1.7	212.4±6.9	4.4	5.82
16	$R^1=R^2=H$, $R^3=OH$	36.3±2.9	59.8±6.9	1.6	4.24

The basic structure and side moieties are shown in Figure S4.
a: Fifty percent effective concentration based on the inhibition of HCV replication.
b: Fifty percent cytotoxicity concentration based on the reduction in cell viability.
c: Selectivity index (CC_{50}/EC_{50}).
d: Determined with ChemDraw software (Chem Bio Office Ultra, 2008).
doi:10.1371/journal.pone.0082299.t004

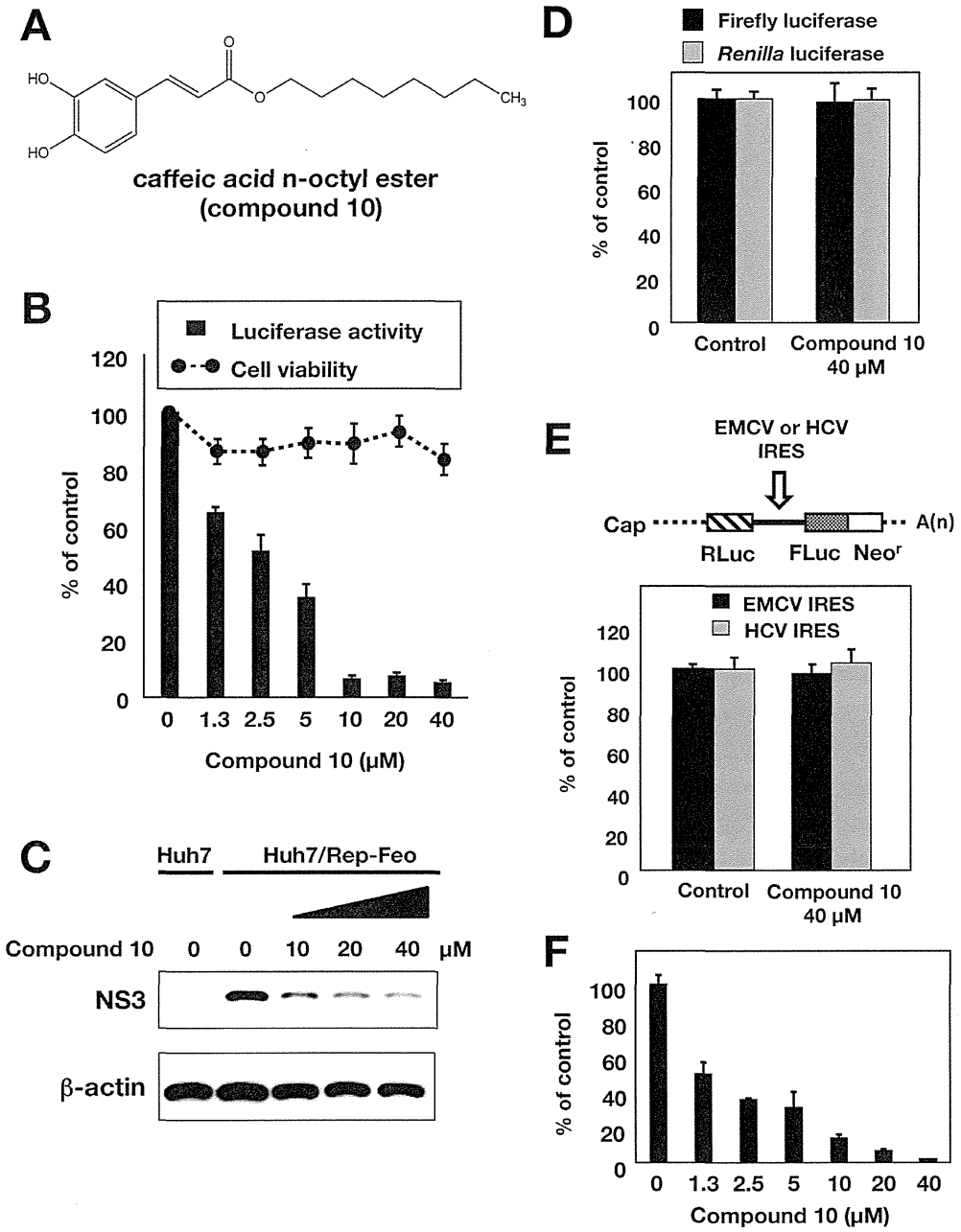

Figure 3. Effect of compound 10 on the viral replication in the replicon cell line and HCVcc. (A) Molecular structure of compound **10**. (B) Huh7/Rep-Feo cells were incubated for 72 h in a medium containing various concentrations of compound **10**. Luciferase and cytotoxicity assays were carried out by the method described in Materials and Methods. Error bars indicate standard deviation. The data represent three independent experiments. (C) Protein extract was prepared from Huh7/Rep-Feo cells treated for 72 h with the indicated concentration of compound **10** and it was then subjected to Western blotting using antibodies to NS3 and beta-actin. (D) Huh7 cell line was transfected with pEF Fluc IN encoding firefly luciferase or pEF Rluc IN encoding *Renilla* luciferase. Both transfected cell lines were incubated with DMSO (Control) or 40 μg/ml compound **10**. Firefly or *Renilla* luciferase activity was measured 72 h post-treatment. Luciferase activity was normalized with protein concentration. Error bars indicate standard deviation. The data were represented from three independent experiments. (E) Schematic structure of RNA transcribed from the plasmids was shown (Top). The bicistronic gene is transcribed under the control of elongation factor 1α (EF1α) promoter. The upstream cistron encoding *Renilla* luciferase (RLuc) is translated by a cap-dependent mechanism. The downstream cistron encodes the fusion protein (Feo), which consists of the firefly luciferase (Fluc) and neomycin phosphotransferase (Neo^r), and is translated under the control of the EMCV or HCV IRES. Huh7 cell line was transfected with each plasmid and incubated for 72 h post-treatment with DMSO (control) or 40 μg/ml of compound **10**. Firefly and *Renilla* luciferase activities were measured. Relative ratio of Firefly luciferase activity to *Renilla* luciferase activity was represented as percentage of the control condition. Error bars indicate standard deviation. The data were represented from three independent experiments. (F) Huh7 OK1 cell line was infected with HCVcc derived from JFH-1 strain and then treated with several concentrations of compound **10** at 24 h post-infection. The resulting cells were harvested 72 h post-infection. The viral RNA of supernatant was purified and estimated by the method described in Materials and Methods. Error bars indicate standard deviation. The data represent three independent experiments. Treatment with DMSO corresponds to '0'.
doi:10.1371/journal.pone.0082299.g003

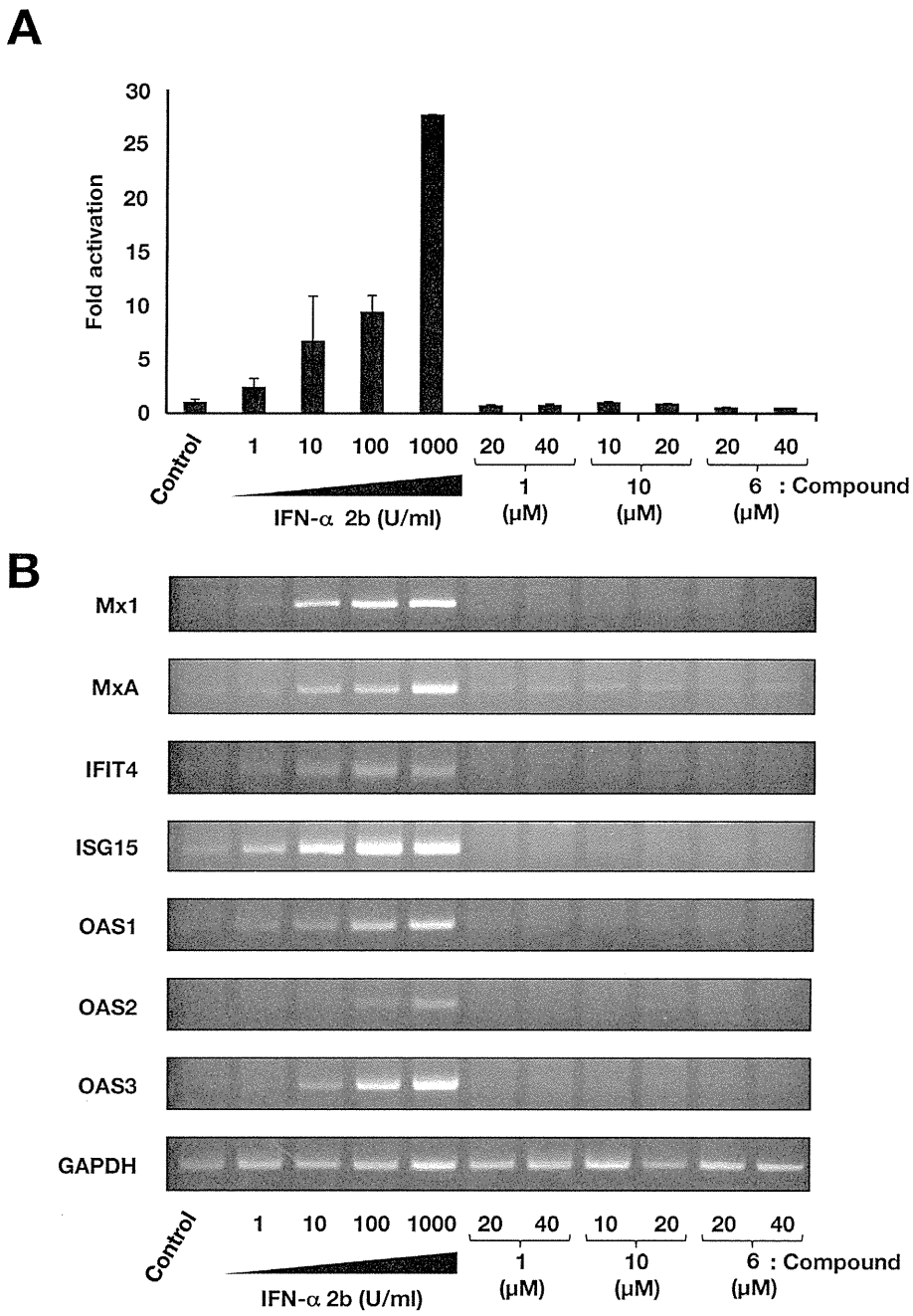

Figure 4. Effect of CAPE derivatives on the interferon-signaling pathway. (A) Plasmids pISRE-TA-Luc and phRG-TK were co-transfect into Huh7 OK1 cells. The transfected cells were cultured with 1, 10, 100, or 1000 U/mL of interferon-alpha 2b, and compounds **1**, **6** and **10**. Treatment with DMSO corresponds to '0'. After 48 h of treatment, luciferase activities were measured, and the value were normalized against *Renilla* luciferase activities. Error bars indicate standard deviation. The data represent three independent experiments. (B) Huh7 replicon cell line of genotype 1b was treated with 1, 10, 100, or 1000 U/mL of interferon-alpha 2b, and compounds **1**, **6** and **10** for 48 h. Treatment with DMSO corresponds to the control. The mRNAs of Mx1, MxA, IFIT4, ISG15, OAS1, OAS2, OAS3, and GAPDH as an internal control were detected by RT-PCR.
doi:10.1371/journal.pone.0082299.g004

of combination tests suggest that daclatasvir, IFN-alpha 2b, and VX-222 synergistically, but telaprevir and danoprevir antagonistically, inhibit HCV replication in combination with compound **10**.

Discussion

CAPE is an active component of propolis, which possesses broad-spectrum biological activities [14–19]. In this study, CAPE suppressed HCV RNA replication in a dose-dependent manner (Fig. 1A and B). Treatment with CAPE inhibited HCV replication with an EC_{50} of 9.0 μM and an SI of 17.9 in Huh7/Rep-Feo cells (Table 1). The treatment of the replicon cell line with CAPE did not induce expression of the IFN-inducible gene (Fig. 4), suggesting that the inhibition of HCV replication by CAPE is independent of the IFN signaling pathway.

Table 5. Anti-HCV activity of compound **10** in replicon cell lines of genotypes 1b and 2a.

Cell line	Replicon type	Strain (Genotype)	EC_{50} [a] (μM)	CC_{50} [b] (μM)	SI [c]
Huh7 Rep/Feo-1b	Subgenome	N (1b)	2.7±0.1	71.7±8.5	26.6
Con1 LUN Sb #26	Subgenome	Con1 (1b)	1.0±0.1	63.1±3.1	63.1
Huh7 Rep/Reo-2a	Subgenome	JFH1 (2a)	1.0±0.3	60.0±2.3	60.0
OR6	Full genome	O (1b)	1.5±0.4	61.7±0.6	41.1

a: Fifty percent effective concentration based on the inhibition of HCV replication.
b: Fifty percent cytotoxicity concentration based on the inhibition of HCV replication.
c: Selectivity Index (CC_{50}/EC_{50}).
doi:10.1371/journal.pone.0082299.t005

We also examined the effect of CAPE derivatives on HCV replication. Our data suggest that the n-alkyl side chain and catechol moiety of the CAPE derivative are critical in its anti-HCV activity (Tables 2 and 3). The EC_{50} value of the derivative decreased dependently on the length of the n-alkyl side chain until reaching octyl ester length (Table 2), while longer chains than octyl ester of a derivative led to an increase in the EC_{50} value and *C*log *P* value. Compound **10**, Caffeic acid n-octyl ester, exhibited the highest anti-HCV activity among the tested compounds with an EC_{50} value of 2.7 μM and an SI value of 26.6. Cyclosporine A and its analogues could suppress the viral replication of genotype 1b at a higher level than that of genotype 2a [23]. Interestingly, compound **10** could inhibit HCV replication of genotype 1b and 2a at a similar level, irrespective of expression of the interferon-inducible gene (Fig. 4). CAPE and its derivatives may therefore possess a mechanism different from cyclosporine A and its analogues with respect to anti-HCV activity.

CAPE has been reported to be an inhibitor of NF-kappaB [14,20]. Lee et al. reported that the catechol moiety in CAPE was important for inhibition of NF-kappaB activation [24]. The data shown in Table 3 suggest that the catechol moiety in CAPE is critical to the anti-HCV activity of compound **10**. Previous studies have implicated the inhibition of NF-kappaB in anti-HCV activity. Treatment with an extract prepared from *Acacia confusa* [25] or San-Huang-Xie-Xin-Tang [26] could suppress HCV replication and inhibit NF-kappaB activation. However, Chen et al. reported that curcumin-mediated inhibition of NF-kappaB did not contribute to anti-HCV activity [11]. Furthermore, treatment with *N*′-(Morpholine-4carbonyloxy)-2(naphthalene-1-yl) acetimidamide could activate NF-kappaB and downstream gene expression in the same Huh7/Rep-Feo replicon cell line as the cell line used in this study and exhibited potent inhibition of HCV replication without interferon signaling [27]. These reports support the notion that CAPE derivatives do not mainly target NF-kappaB activity as part of their anti-HCV activity.

Several host proteins have been reported to regulate function of NS5A, leading to supporting HCV replication (review in [2,28]). Daclatasvir exhibited potent synergistic effect on anti-HCV activity in combination of compound **10** (Fig. 5). Anti-HCV activity of compound **10** might associate with intrinsic functions of host factors that interact with NS5A. NS3 protease inhibitors exhibited antagonistic effect in combination of compound **10** (Fig. 5). The inhibitory effect of compound **10** might be mediated by the activation of an unknown endogenous protease that is nonspecifically suppressed by NS3 protease inhibitors. Further study to clarify the mechanism by which compound **10** suppresses HCV replication might contribute to identification of a novel host factor as a drug target for development of the effective compound supporting an effect of other anti-HCV drugs.

In conclusion, we showed that CAPE and its analogue possess a significant inhibitory effect against HCV replication. The length of n-alkyl side chains and the catechol moiety of CAPE are critical to its inhibitory activity against HCV replication. The most effective derivative among the tested compounds was caffeic acid n-octyl ester, which exhibited an EC_{50} value of 1 μM and an SI value of 63.1 in the replicon cell line of genotype 1b strain Con1. Treatment with caffeic acid n-octyl ester reduced the viral replication of genotype 1b and 2a at a similar level and inhibited viral production of HCVcc. Treatment with caffeic acid n-octyl ester could synergistically enhance the anti-HCV activities of IFN-α 2b, daclatasvir, and VX-222, but neither telaprevir nor danoprevir. Further investigation to clarify the mechanism of anti-HCV activity and further modification of the compound to improve anti-HCV activity will lead to novel therapeutic strategies to treat chronic hepatitis C virus infection.

Materials and Methods

Compounds

Boldface numbers in this text indicate the compound numbers shown in Tables. All chemical structures of compounds used in this study are shown in figure S1. CAPE (**1**), caffeic acid (**2**), ferulic acid (**3**), and chlorogenic acid (**5**) and were purchased from Sigma-Aldrich (St. Louis, MO, USA). Cinnamic acid phenethyl ester (**4**) was from Tokyo Chemical Industry (Tokyo, Japan). Rosmarinic acid (**6**) was from Wako Pure Chemical (Tokyo, Japan). Caffeic acid n-octyl ester (n-octyl caffeate) (**10**), 3-O-methylcaffeic acid n-octyl ester (n-octyl-3-methylcaffeate) (**13**), 4-O-methylcaffeic acid n-octyl ester (n-octyl-3-methylcaffeate) (**14**), and 3, 4-O-dimethyl-caffeic acid n-octyl ester (n-octyl-3, 4-methylcaffeate) (**15**) were from LKT Laboratories (St. Paul, MN, USA).

Caffeic acid esters **7**, **8**, **9**, and **11** were synthesized by preparing caffeic acid chloride followed by treatment with corresponding alcohols [29]. Dihydrocaffeic acid ester **12** was prepared by hydrogenation of **7**. Compound **16** is a newly synthesized ester. Spectroscopic data of known esters **7–9**, and **11** prepared here were identical to those reported [30-32] Interferon alfa-2b (IFN-α 2b) was obtained from MSD (Tokyo, Japan). Telaprevir and daclatasvir were purchased from Selleckchem (Houston, TX, USA). Danoprevir and VX-222 were from AdooQ BioScience (Irvine, CA, USA).

Chemistry of 3,4,5-Trihydroxycinnamic acid n-octyl ester

3,4,5-Trihydroxycinnamic acid n-octyl ester (**16**) was prepared by condensation of corresponding benzaldehydes with malonic acid n-octyl monoester [33]. A solution of malonic acid n-octyl monoester (432 mg, 2 mmol), 3,4,5-trihydroxybenzaldehyde (462 mg, 3 mmol) and piperidine (0.2 mL) in pyridine (2 mL)

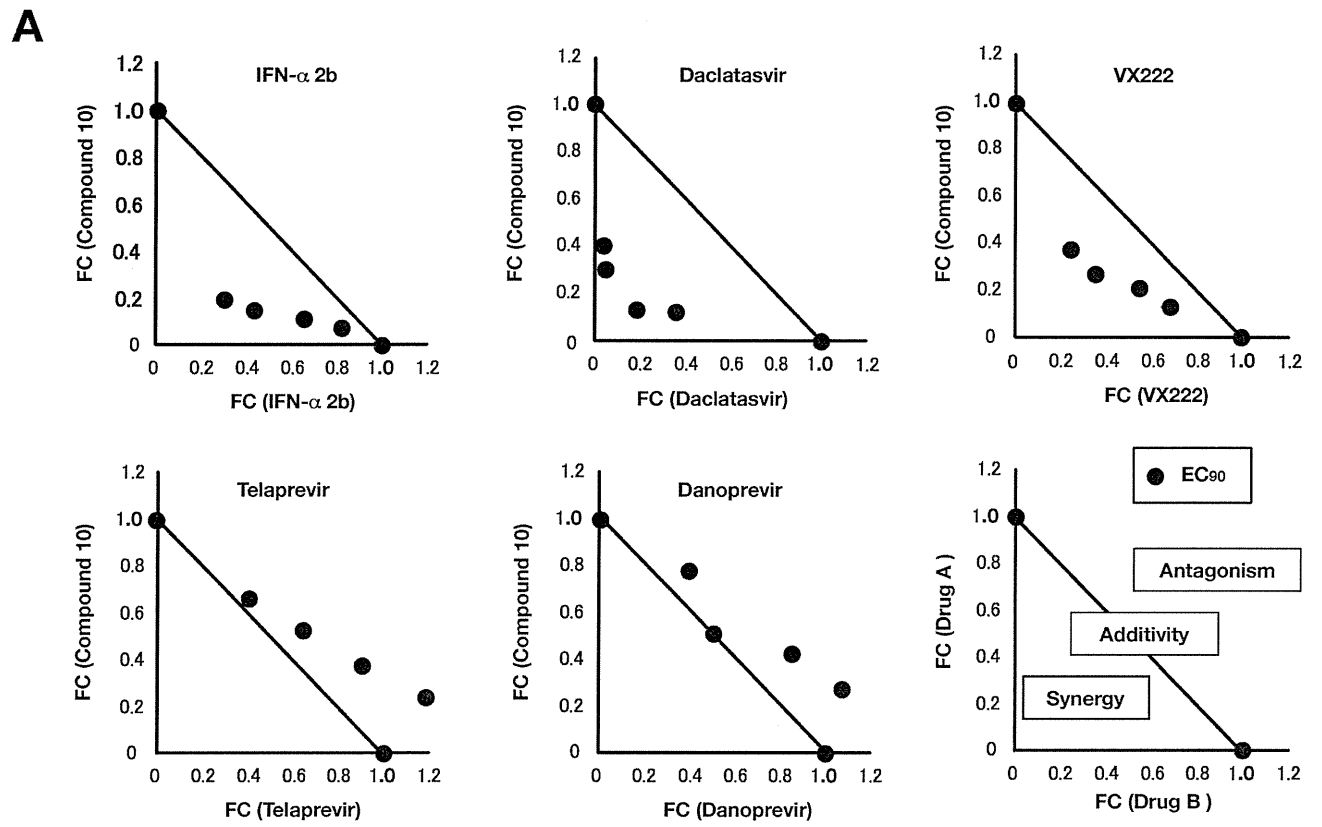
A
IFN-α 2b
FC (Compound 10)
FC (IFN-α 2b)
Daclatasvir
FC (Daclatasvir)
VX222
FC (VX222)
Telaprevir
FC (Telaprevir)
Danoprevir
FC (Danoprevir)
EC90
Antagonism
Additivity
Synergy
FC (Drug A)
FC (Drug B)

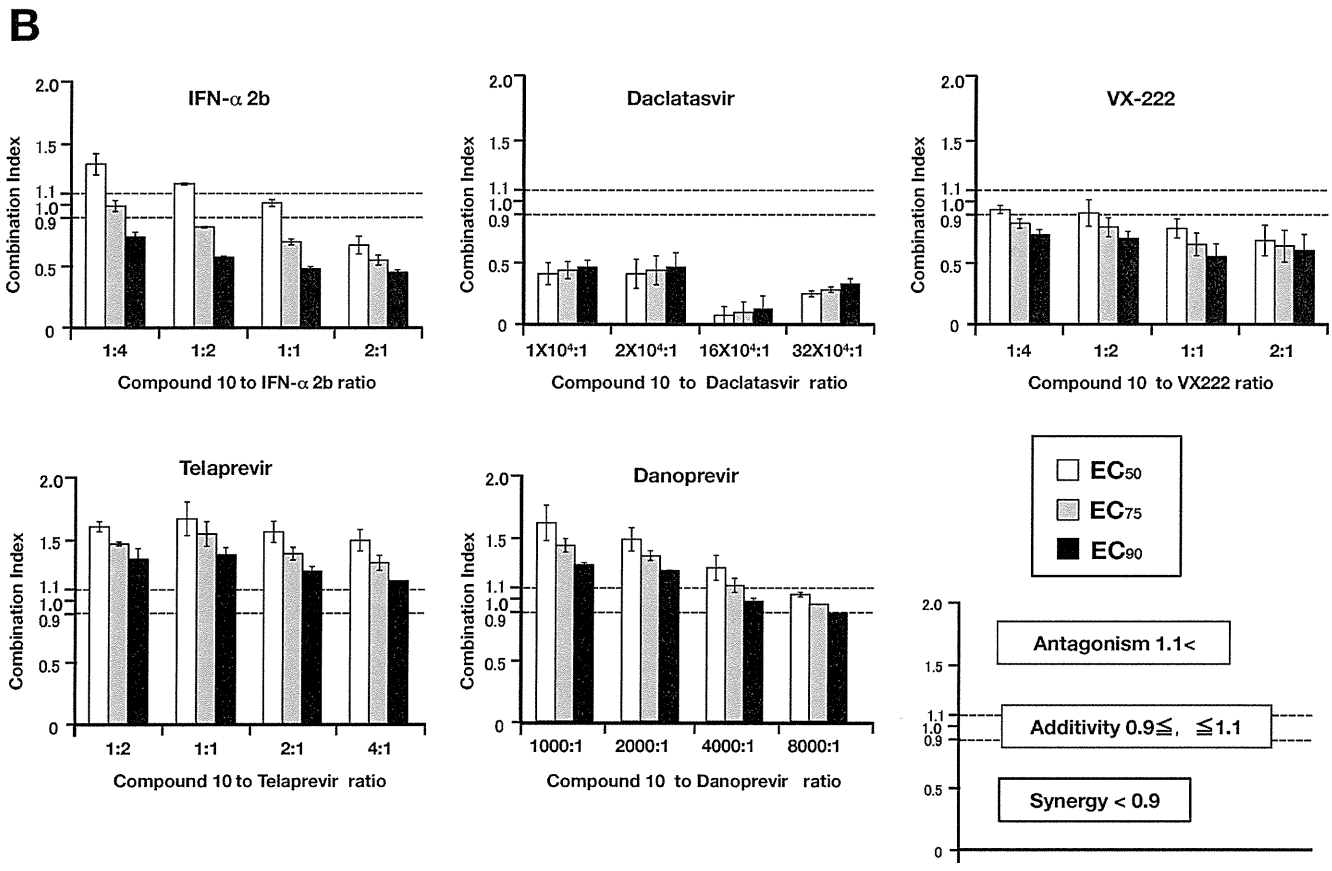
B
IFN-α 2b
Combination Index
1:4
1:2
1:1
2:1
Compound 10 to IFN-α 2b ratio
Daclatasvir
1X10⁴:1
2X10⁴:1
16X10⁴:1
32X10⁴:1
Compound 10 to Daclatasvir ratio
VX-222
Compound 10 to VX222 ratio
Telaprevir
1:2
1:1
2:1
4:1
Compound 10 to Telaprevir ratio
Danoprevir
1000:1
2000:1
4000:1
8000:1
Compound 10 to Danoprevir ratio
EC50
EC75
EC90
Antagonism 1.1<
Additivity 0.9≦, ≦1.1
Synergy < 0.9

Figure 5. Synergistic effect analyses for the combination of compound 10 with IFN-α 2b, daclatasvir, VX-222, telaprevir, or danoprevir. The Huh7 cell line, including the subgenomic replicon RNA of genotype 1b strain Con1, was treated for 72h with combinations of compound 10 and IFN-α 2b, daclatasvir, VX-222, telaprevir, or danoprevir. Luciferase assay were carried out as described in Materials and Methods. (A) The calculated EC_{90} values for combination were plotted as the fractional concentration (FC) of compound 10 and one of IFN-α 2b, daclatasvir, VX-222, telaprevir, and danoprevir on the *x* and *y* axes, respectively. Synergy, antagonism and additivity are indicated in a representative graph as a right end of lower graphs and are described in Materials and Methods. (B) Combination indexes of compound 10 with IFN-α 2b, daclatasvir, VX-222, telaprevir, or danoprevir at the EC50, EC75, and EC90 values were measured at various drug rations. Synergy, antagonism and additivity are indicated in a representative graph as a right end of lower graphs and are described in Materials and Methods.
doi:10.1371/journal.pone.0082299.g005

was heated at 70°C for 1 h. The reaction mixture was concentrated under a vacuum to give a residue, which was dissolved in $CHCl_3$-IPA (3:1, v/v) and then washed with 10% HCl and water. The organic layer was dried over Na_2SO_4 and evaporated to give a residue, which was purified by silica gel column chromatography using AcOEt-hexane (1:1, v/v) as eluent to give the corresponding n-octyl ester (85 mg, 13.8%) as a pale powder. FT-IR νmax (KBr): 3389, 3239, 2923, 1675, 1627, 1606 cm^{-1}. ^1H NMR (400MHz, CD_3OD) δ: 0.86 (3H, t, J = 7.2 Hz), 1.20–1.40 (10H, m), 1.65 (2H, quintet, J = 6.4 Hz), 4.11, (2H, t, J = 6.4 Hz), 6.16 (2H, d, J = 15.6 Hz), 6.55 (2H, s), 7.40 (2H, d, J = 15.6 Hz). 13C NMR (100 Hz, CD_3OD) δ: 14.4, 23.7, 27.1, 29.8, 30.3, 30.4, 32.9, 65.6, 108.5, 115.3, 126.6, 137.5, 147.1, 169.4. CI MS *m/z*: 309 (M^++H). High-resolution CI MS calcd. for $C_{17}H_{25}O_5$ (M^++H) for 309.1702. Found: 309.1686.

Replicon cell lines and virus infection

The Huh7/Rep-Feo cell line, which harbors the subgenomic replicon RNA composed of HCV IRES, the gene of the fusion protein consisting of neomycin phosphotransferase and firefly luciferase, EMCV IRES and a nonstructural gene of genotype 1b strain N in order in Huh7 cell line, was previously established [34]. Thus, the luciferase activity corresponds to the level of HCV RNA replication. The cell line was maintained in Dulbecco's modified Eagle medium containing 10% fetal calf serum and 0.5 mg/mL G418 and cultured in absence of G418 when they were treated with compounds. The Lunet/Con1LUN Sb #26 cell line, which harbors the subgenomic replicon RNA of the Con1 strain (genotype 1b), was described previously [35]. The OR6 cell line, which harbors the full genomic replicon RNA of the O strain (genotype 1b), was described previously [36]. The HCV replicon cell line derived from the genotype 2a strain JFH1 was described previously [37]. The viral RNA derived from the plasmid pJFH1 was transcribed and introduced into Huh7OK1 cells according to the method of Wakita et al. [38]. The virus was amplified by the several times passages. The cells were infected with the virus at a multiplicity of infection (moi) of 1 and then treated with each compound at 24 h post-infection. The culture supernatants were harvested 72 h post-treatment to estimate the viral RNA as described below.

Determination of luciferase activity in HCV replicon cells

The replicon cells were seeded at 2×10^4 cells per well in a 48-well plate 24 h before treatment. Compounds were added to the culture medium to give various concentrations. The resulting cells were harvested 72 h post-treatment and lysed with cell culture lysis reagent (Promega, Madison, WI). The luciferase activity of each cell lysate was estimated using a luciferase assay system (Promega). The resulting luminescence was detected by a Luminescencer-JNR AB-2100 (ATTO, Tokyo, Japan).

Determination of Cytotoxicity in HCV replicon cells

The replicon cells were seeded at a density of 1×10^4 cells per well in a 96-well plate and then incubated at 37°C for 24 h. Compounds were added to the culture medium to give various concentrations and were then harvested 72 h post-treatment. Cell viability was measured using a dimethylthiazol carboxymethoxyphenylsulfophenyl tetrazolium (MTS) assay with a CellTiter 96 aqueous one-solution cell proliferation assay kit (Promega).

Western Blotting

Western blotting was carried out by the method described previously [39]. The antibodies to NS3 (clone 8G-2, mousemonoclonal, Abcam, Cambridge, UK), and beta-actin were purchased from Cell Signaling Technology (rabbit polyclonal, Danvers, MA, USA) and were used as the primary antibodies in this study.

RNA analysis

Total RNAs were prepared from cells by using the RNAqueous-4PCR kit (Life Technologies, Carlsbad, CA). Viral RNA were prepared from culture supernatants by using the QIAamp Viral RNA mini kit (QIAGEN, Hilden, Germany). The viral RNA genome was estimated by the qRT-PCR method described previously [40]. RT-PCR was carried out by the method described previously [41] which was slightly modified at the PCR step. The PCR samples were incubated once for 10 min at 95°C for an initial activation step of the AmpliTaq Gold DNA Polymerase (Life Technologies), and then subjected to an amplification step of 30 repeats of the cycle consisting of three segments as follow: 0.5 min at 95°C, 1 min at 55°C and 1 min at 72°C. The primers used in this study were as follows: Mx1: 5′-AGCCACTGGACTGACGACTT-3′ and 5′-GAGGGCTGAAAATCCCTTTC-3′;

MxA: 5′-GTCAGGAGTTGCCCTTCCCA-3′ and 5′-ATTCCCATTCCTTCCCCGG-3′;

IFIT4: 5′-CCCTTCAGGCATAGGCAGTA-3′ and 5′-CTCCTACCCGTCACAACCAC -3′; ISG15: 5′-CGCAGATCACCCAGAAGAT-3′ and 5′-GCCCTTGTTATTCCTCACCA-3′;

OAS1: 5′-CAAGCTCAAGAGCCTCATCC-3′ and 5′-TGGGCTGTGTTGAAATGTGT-3′;

OAS2: 5′-ACAGCTGAAAGCCTTTTGGA-3′ and 5′-GCATTAAAGGCAGGAAGCAC-3′;

OAS3: 5′-CACTGACATCCCAGACGATG-3′ and 5′-GATCAGGCTCTTCAGCTTGGC-3′;

GAPDH: 5′-GAAGGTGAAGGTCGGAGTC and 5′- GAAGATGGTGATGGGATTTC-3′

Effects on activities of internal ribosome entry site (IRES) and luciferases

Huh7 OK1 cells were transfected with pEF.Rluc.HCV.IRES.-Feo or pEF.Rluc.EMCV.IRES.Feo [39]. These transfected cells were seeded at 2×10^4 cells per well in a 48-well plate 24 h before treatment, treated with DMSO or compound **10**, and then harvested at 72 h post-treatment. The firefly luciferase activities were measured with a luciferase assay system (Promega). The total protein concentration was measured using the BCA Protein Assay Reagent Kit (Thermo Scientific, Rockford, IL, USA) to normalize

luciferase activity. To evaluate the interferon response, Huh7OK1 cells were seeded on a 48 well plate at a density of 2×10^4 cells per well, and transfected with pISRE-TA-Luc (Takara bio, Shiga, Japan) and phRG-TK (Promega). These transfected cells were incubated in the presence of compounds, IFN-α 2b, or DMSO, and then harvested at 48 h post-treatment. The firefly luciferase and *Renilla* luciferase activities were quantified by using Dual luciferase reporter assay system (Promega).

Prediction of Clog*P* for compounds

The *Clog*P value deduced from chemical structure roughly corresponds to a value of hydrophobicity. The *Clog*P values of compounds used in this study were calculated using the computer software Chem Bio Office Ultra 2008 (PerkinElmer, Cambridge, MA, USA).

Synergistic effect of caffeic acid n-octyl ester on anti-HCV activities of other drugs

The effects of drug-drug combinations were evaluated by using the Con1 LUN Sb #26 replicon cells, and were analyzed by using the computer software CalcuSyn (Biosoft, Cambridge, United Kingdom). Dose inhibition curves of two different drugs were plotted with each other. In each drug combination, EC_{90} values of several combinations of two different drugs were plotted as the fractional concentration (FC) of both drugs on the *x* and *y*-axes. Additivity indicates the line linked between 1.0 FC value points of both drugs in the absence of each other. Synergy and antagonism are indicated by values plotted under and above, respectively, an additivity line. The explanatory diagram of isobologram is shown in a right end of lower panels of Figure 5A. Combination indexes (CIs) were calculated at the EC_{50}, EC_{75}, and EC_{90} by using CalcuSyn. A CI value of less than 0.9 indicates synergy. A CI value ranging from 0.9 to 1.1 indicates additivity. A CI value of more than 1.1 indicates antagonism. The explanatory diagram was shown in a right end of lower panels of Figure 5B.

Supporting Information

Figure S1 Molecular structure of CAPE and commercial CAPE-related compounds. CAPE structure is divided into three parts: (I) the catechol moiety, (II) the alkenyl moiety on alpha, beta -unsaturated ester, and (III) the ester part. Molecular structures of CAPE and its commercial derivatives are shown.
(TIF)

Figure S2 The basic structure and side moieties of compounds shown in Table 2. Each compound structure is represented on the basis of the basic structure (top).
(TIF)

Figure S3 The molecular structures of compounds 7 and 12, which are shown in Table 3. Both compounds are different in alpha, beta-unsaturated or saturated part attached to ester.
(TIF)

Figure S4 The basic structure and side moieties of compounds shown in Table 4. Each compound structure is represented on the basis of the basic structure (top).
(TIF)

Acknowledgments

We thank T. Wakita for kindly providing a plasmid.

Author Contributions

Conceived and designed the experiments: MT KM. Performed the experiments: H. Shen AY MN HY MS H. Shindo SM. Analyzed the data: HK TT NE. Contributed reagents/materials/analysis tools: YF MI NK NS. Wrote the paper: H. Shen AY MT KM.

References

1. Baldo V, Baldovin T, Trivello R, Floreani A (2008) Epidemiology of HCV infection. Curr Pharm Des 14: 1646–1654.
2. Moriishi K, Matsuura Y (2012) Exploitation of lipid components by viral and host proteins for hepatitis C virus infection. Front Microbiol 3: 54.
3. Hijikata M, Kato N, Ootsuyama Y, Nakagawa M, Shimotohno K (1991) Gene mapping of the putative structural region of the hepatitis C virus genome by in vitro processing analysis. Proc Natl Acad Sci USA 88: 5547–5551.
4. Lohmann V, Korner F, Koch J, Herian U, Theilmann L, et al. (1999) Replication of subgenomic hepatitis C virus RNAs in a hepatoma cell line. Science 285: 110–113.
5. Hofmann WP, Zeuzem S (2011) A new standard of care for the treatment of chronic HCV infection. Nat Rev Gastroenterol Hepatol 8: 257–264.
6. Jacobson IM, McHutchison JG, Dusheiko G, Di Bisceglie AM, Reddy KR, et al. (2011) Telaprevir for previously untreated chronic hepatitis C virus infection. N Engl J Med 364: 2405–2416.
7. Sarrazin C, Hezode C, Zeuzem S, Pawlotsky JM (2012) Antiviral strategies in hepatitis C virus infection. J Hepatol 56 Suppl 1: S88–100.
8. Kieffer TL, Kwong AD, Picchio GR (2010) Viral resistance to specifically targeted antiviral therapies for hepatitis C (STAT-Cs). J Antimicrob Chemother 65: 202–212.
9. Ahmed-Belkacem A, Ahnou N, Barbotte L, Wychowski C, Pallier C, et al. (2010) Silibinin and related compounds are direct inhibitors of hepatitis C virus RNA-dependent RNA polymerase. Gastroenterology 138: 1112–1122.
10. Calland N, Albecka A, Belouzard S, Wychowski C, Duverlie G, et al. (2012) (-)-Epigallocatechin-3-gallate is a new inhibitor of hepatitis C virus entry. Hepatology 55: 720–729.
11. Chen MH, Lee MY, Chuang JJ, Li YZ, Ning ST, et al. (2012) Curcumin inhibits HCV replication by induction of heme oxygenase-1 and suppression of AKT. Int J Mol Med 30: 1021–1028.
12. Bachmetov L, Gal-Tanamy M, Shapira A, Vorobeychik M, Giterman-Galam T, et al. (2012) Suppression of hepatitis C virus by the flavonoid quercetin is mediated by inhibition of NS3 protease activity. J Viral Hepat 19: e81–88.
13. Takeshita M, Ishida Y, Akamatsu E, Ohmori Y, Sudoh M, et al. (2009) Proanthocyanidin from blueberry leaves suppresses expression of subgenomic hepatitis C virus RNA. J Biol Chem 284: 21165–21176.
14. Toyoda T, Tsukamoto T, Takasu S, Shi L, Hirano N, et al. (2009) Anti-inflammatory effects of caffeic acid phenethyl ester (CAPE), a nuclear factor-kappaB inhibitor, on Helicobacter pylori-induced gastritis in Mongolian gerbils. Int J Cancer 125: 1786–1795.
15. Ho CC, Lin SS, Chou MY, Chen FL, Hu CC, et al. (2005) Effects of CAPE-like compounds on HIV replication in vitro and modulation of cytokines in vivo. J Antimicrob Chemother 56: 372–379.
16. Chiao C, Carothers AM, Grunberger D, Solomon G, Preston GA, et al. (1995) Apoptosis and altered redox state induced by caffeic acid phenethyl ester (CAPE) in transformed rat fibroblast cells. Cancer Res 55: 3576–3583.
17. Boudreau LH, Maillet J, LeBlanc LM, Jean-Francois J, Touaibia M, et al. (2012) Caffeic acid phenethyl ester and its amide analogue are potent inhibitors of leukotriene biosynthesis in human polymorphonuclear leukocytes. PLoS One 7: e31833.
18. Lee KW, Chun KS, Lee JS, Kang KS, Surh YJ, et al. (2004) Inhibition of cyclooxygenase-2 expression and restoration of gap junction intercellular communication in H-ras-transformed rat liver epithelial cells by caffeic acid phenethyl ester. Ann N Y Acad Sci 1030: 501–507.
19. Fesen MR, Kohn KW, Leteurtre F, Pommier Y (1993) Inhibitors of human immunodeficiency virus integrase. Proc Natl Acad Sci U S A 90: 2399–2403.
20. Natarajan K, Singh S, Burke TR Jr, Grunberger D, Aggarwal BB (1996) Caffeic acid phenethyl ester is a potent and specific inhibitor of activation of nuclear transcription factor NF-kappa B. Proc Natl Acad Sci U S A 93: 9090–9095.
21. Li Y, Zhang T, Douglas SD, Lai JP, Xiao WD, et al. (2003) Morphine enhances hepatitis C virus (HCV) replicon expression. Am J Pathol 163: 1167–1175.
22. Okamoto T, Omori H, Kaname Y, Abe T, Nishimura Y, et al. (2008) A single-amino-acid mutation in hepatitis C virus NS5A disrupting FKBP8 interaction impairs viral replication. J Virol 82: 3480–3489.
23. Ishii N, Watashi K, Hishiki T, Goto K, Inoue D, et al. (2006) Diverse effects of cyclosporine on hepatitis C virus strain replication. J Virol 80: 4510–4520.

24. Lee Y, Shin DH, Kim JH, Hong S, Choi D, et al. (2010) Caffeic acid phenethyl ester-mediated Nrf2 activation and IkappaB kinase inhibition are involved in NFkappaB inhibitory effect: structural analysis for NFkappaB inhibition. Eur J Pharmacol 643: 21–28.
25. Lee JC, Chen WC, Wu SF, Tseng CK, Chiou CY, et al. (2011) Anti-hepatitis C virus activity of Acacia confusa extract via suppressing cyclooxygenase-2. Antiviral Res 89: 35–42.
26. Lee JC, Tseng CK, Wu SF, Chang FR, Chiu CC, et al. (2011) San-Huang-Xie-Xin-Tang extract suppresses hepatitis C virus replication and virus-induced cyclooxygenase-2 expression. J Viral Hepat 18: e315–324.
27. Kusano-Kitazume A, Sakamoto N, Okuno Y, Sekine-Osajima Y, Nakagawa M, et al. (2012) Identification of novel N-(morpholine-4-carbonyloxy) amidine compounds as potent inhibitors against hepatitis C virus replication. Antimicrob Agents Chemother 56: 1315–1323.
28. Moradpour D, Penin F, Rice CM (2007) Replication of hepatitis C virus. Nat Rev Microbiol 5: 453–463.
29. Lee YJ, Liao PH, Chen WK, Yang CY (2000) Preferential cytotoxicity of caffeic acid phenethyl ester analogues on oral cancer cells. Cancer Lett 153: 51–56.
30. Bourne GT, Golding SW, McGeary RP, Meutermans WD, Jones A, et al. (2001) The development and application of a novel safety-catch linker for BOC-based assembly of libraries of cyclic peptides. J Org Chem 66: 7706–7713.
31. Nagaoka T, Banskota AH, Tezuka Y, Saiki I, Kadota S (2002) Selective antiproliferative activity of caffeic acid phenethyl ester analogues on highly liver-metastatic murine colon 26-L5 carcinoma cell line. Bioorg Med Chem 10: 3351–3359.
32. Uwai K, Osanai Y, Imaizumi T, Kanno S, Takeshita M, et al. (2008) Inhibitory effect of the alkyl side chain of caffeic acid analogues on lipopolysaccharide-induced nitric oxide production in RAW264.7 macrophages. Bioorg Med Chem 16: 7795–7803.
33. Zhang Z, Xiao B, Chen Q, Lian XY (2010) Synthesis and biological evaluation of caffeic acid 3,4-dihydroxyphenethyl ester. J Nat Prod 73: 252–254.
34. Yokota T, Sakamoto N, Enomoto N, Tanabe Y, Miyagishi M, et al. (2003) Inhibition of intracellular hepatitis C virus replication by synthetic and vector-derived small interfering RNAs. EMBO Rep 4: 602–608.
35. Frese M, Barth K, Kaul A, Lohmann V, Schwarzle V, et al. (2003) Hepatitis C virus RNA replication is resistant to tumour necrosis factor-alpha. Journal of General Virology 84: 1253–1259.
36. Ikeda M, Abe K, Dansako H, Nakamura T, Naka K, et al. (2005) Efficient replication of a full-length hepatitis C virus genome, strain O, in cell culture, and development of a luciferase reporter system. Biochem Biophys Res Commun 329: 1350–1359.
37. Nishimura-Sakurai Y, Sakamoto N, Mogushi K, Nagaie S, Nakagawa M, et al. (2010) Comparison of HCV-associated gene expression and cell signaling pathways in cells with or without HCV replicon and in replicon-cured cells. J Gastroenterol 45: 523–536.
38. Wakita T, Pietschmann T, Kato T, Date T, Miyamoto M, et al. (2005) Production of infectious hepatitis C virus in tissue culture from a cloned viral genome. Nat Med 11: 791–796.
39. Yamashita A, Salam KA, Furuta A, Matsuda Y, Fujita O, et al. (2012) Inhibition of hepatitis C virus replication and NS3 helicase by the extract of the feather star *Alloeocomatella polycladia*. Mar Drugs 10: 744–761.
40. Fujimoto Y, Salam KA, Furuta A, Matsuda Y, Fujita O, et al. (2012) Inhibition of Both Protease and Helicase Activities of Hepatitis C Virus NS3 by an Ethyl Acetate Extract of Marine Sponge Amphimedon sp. PLoS One 7: e48685.
41. Jin H, Yamashita A, Maekawa S, Yang PT, He LM, et al. (2008) Griseofulvin, an oral antifungal agent, suppresses hepatitis C virus replication in vitro. Hepatology Research 38: 909–918.

第2章 各論

Population-based study 7

地域コホート研究からみたC型肝炎ウイルス持続感染者の自然史

Natural history of persistently infected-hepatitis C virus carrier based on a cohort study in HCV hyperendemic area

渡辺久剛[1]・齋藤貴史[1]・石橋正道[2]・新澤陽英[3]・河田純男[1,4]

山形大学医学部消化器内科学[1]，内科消化器科石橋医院[2]
公立置賜総合病院[3]，兵庫県立西宮病院[4]

キーワード　分子疫学研究，地域コホート，HCV，自然予後，遺伝子多型

要旨

山形大学医学部第二内科(消化器内科)では，1991年からC型肝炎ウイルス(HCV)感染多発地域において住民コホート研究を行ってきた。これまでの解析からは，HCV感染の疫学はもちろんのこと，HCV感染経過と宿主因子の関係，キャリアにおける自然治癒と肝発癌，HCV感染者の生命予後に関する知見が集積され，コホート研究の果たしてきた役割は大きいと思われる。とくに21世紀COEプログラムの一環として行ったHCV感染経過に関わる宿主遺伝子要因探索では，HCV感染感受性やウイルス複製，免疫応答に関与する複数の一塩基多型(SNP)が明らかとなった。わが国ではHCV感染例の高齢化が問題となっており，これら地域コホートを通じたキャリアの病診連携の推進が望まれる。

代表著者連絡先

渡辺久剛
Facsimile：023-628-5311

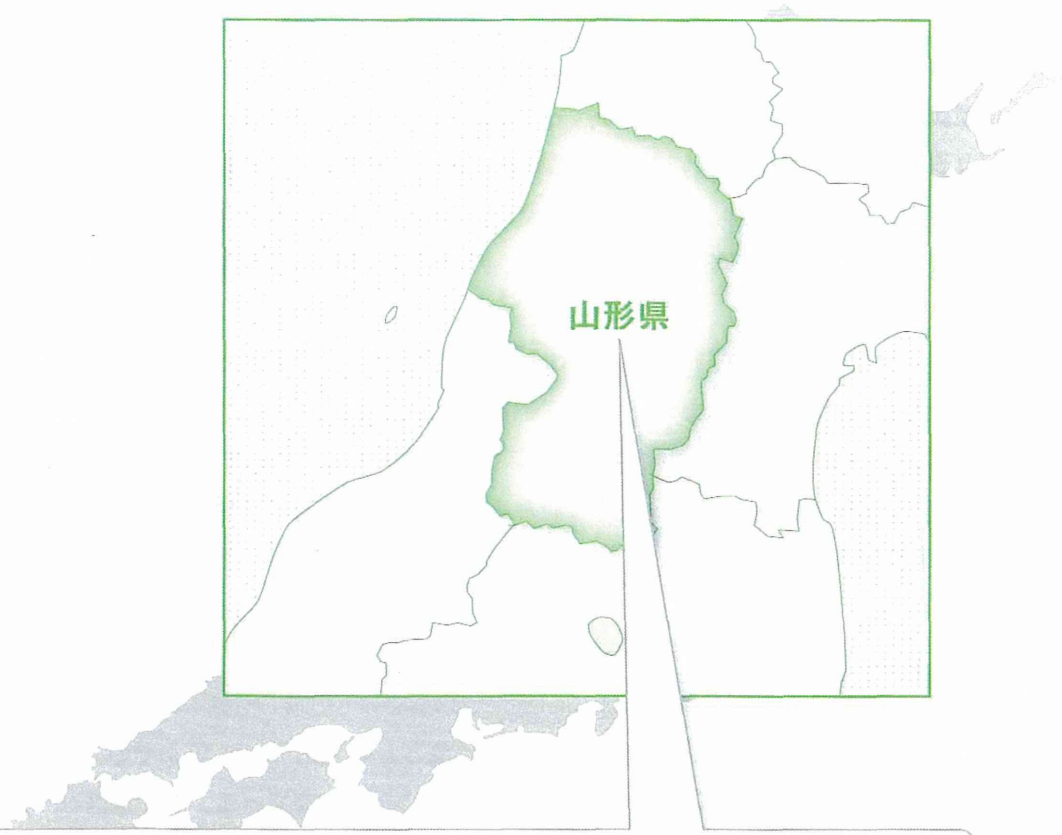

対象となったコホート調査の町に関する基本情報

1990 年秋，新澤陽英先生（当時 山形大学医学部第二内科（消化器内科））から石橋正道先生へ，C 型肝炎ウイルス（HCV）に関する住民検診を担当するよう指示があったと聞いている。新澤先生は当時の予防協会や献血センターのデータから，山形県内に HCV の高浸淫地域が複数存在することを確信していたが，そのため，検診すべき対象自治体が県内複数に及ぶこととなり，以後数年にわたり，肝臓研究班のメンバーは検診業務に忙殺されることとなった。

なかでも現在まで追跡検診が続いている R 町は，県南に位置する人口 15,000 人あまりの自治体であるが，1967～1973 年にかけて河川沿いに急性肝炎が多発したことが当時の新聞記事などで報道されており，真っ先に本検診対象と考えられたことから，翌 1991 年から当教室と R 町役場を中心に町全体の HCV 感染実態調査を行うこととなった。新澤先生を中心とし，山形大学医学部第二内科の肝臓研究班が 5 年の歳月をかけて連日，町内すべての地域内の公民館などをくまなく回り，子供を含む全住民を対象に，採血を含めた感染実態調査を行ったのが現在の山形 HCV コホートの始まりである。

はじめに

C型肝炎ウイルス(hepatitis C virus；HCV)感染者の分布は世界的あるいは国内的に地域的な偏りがある。山形県においてもHCV感染者の地域分布には偏りがあり，高浸淫地域が存在する。そのような地域では，慢性肝臓病の予防のため積極的な医療介入が必要であるが，同時にそのような地域における分子疫学研究は，C型肝炎の未解決の問題を明らかにするうえできわめて重要である。

われわれは1991年より現在に至るまで，C型肝炎をターゲットとしたコホート設定とその追跡調査を行ってきた[1)-3)]。また隣接したN市U地区住民3,814人に対し，1991～1992年にかけて2,382人(62.5%)のHCV感染実態を調査した。本稿では，これまで山形大学医学部第二内科(消化器内科)が行ってきた，長年にわたるHCV感染多発地区住民コホート研究からみえてきたHCV感染の疫学と，自然経過，感染者の予後について紹介したい。

I 山形コホート

本地域コホートは，R町全住民約15,000人を対象とした1991～1995年までのmass surveyと，1996年以降現在まで続くHCV RNA持続陽性者の追跡調査である。この地区は，何十年にもわたり人の出入りがきわめて少ない地区であるため，HCV感染自然史に関わる分子疫学研究に優れた地域と考えられる[4)]。

1991年および1992年は6歳以上の4,655人を対象とし，1993～1995年にかけて30歳以上の住民10,709人に対し調査を行った。この間同時に2,568組の夫婦について，HCVの夫婦間感染実態についても検討した。Mass surveyの受診率は全住民15,364人中8,950人(58.3%)であり，うち1,078人(12%)がHCV抗体(hepatitis C virus antibody；anti-HCV)陽性であった。とくに1967～1973年にかけて原因不明の急性肝炎が多発したA地区では，HCV抗体陽性者は地区住民3,094人中602人(19.5%)に上り，その78.1%でHCV RNAが陽性であることが判明した[3)]。

年齢階層別のHCV抗体陽性率は，40歳未満ではわずか1.4%であるのに対し，40歳以上では32.4%と明らかに高く(図1)，また急性肝炎流行以前より住んでいた住民におけるHCV抗体陽性率は34.7%(559人/1,609人)であり，急性C型肝炎流行後に居住した住民のHCV抗体陽性率(9人/156人；5.8%)と比べ有意に高いことがわかった。検診受診時調査票をもとに感染リスク要因を解析すると，手術歴，輸血歴，鍼治療歴が有意なリスク要因であることが当時の住民コホートから明らかにされた(表1)。